Nanoparticle-induced Changes in Insulin Fibrillation Behavior

A thesis presented to the faculty of

the Russ College of Engineering and Technology of Ohio University

In partial fulfillment of the requirements for the degree

Master of Science

Zahra Khosravi

December 2020

This thesis titled

Nanoparticle-induced Changes in Insulin Fibrillation Behavior

by

ZAHRA KHOSRAVI

has been approved for

the Department of Chemical and Biomolecular Engineering

and the Russ College of Engineering and Technology by

Amir M. Farnoud

Assistant Professor of Chemical Engineering

Mei Wei

Dean, Russ College of Engineering and Technology

Abstract

KHOSRAVI, ZAHRA, M.S., December 2020, Biomedical Engineering

Nanoparticle-induced Changes in Insulin Fibrillation Behavior

Director of Thesis: Amir M. Farnoud

Insulin fibrillation occurs due to the interaction of partially unfolded insulin molecules resulting in the formation of insoluble aggregates known as fibrils. Insulin fibril deposition has been reported at the site of injection after repeated injection occurring in patients with type II diabetes. Fibrillation is also a major issue in pharmaceutical industry for insulin production and purification. Application of engineered nanoparticles has been reported to accelerate or inhibit insulin fibrillation. However, the mechanism by which engineered nanoparticles regulate insulin fibrillation behavior, and the dependence of such mechanisms on particle physicochemical properties, is still not fully understood. In the current study, insulin fibrillation in the presence of amine-modified (223 ± 6 nm) and sulfate-modified (241 ± 12 nm) polystyrene particles was investigated in an effort to elucidate the role of particle surface functional groups on insulin fibrillation behavior.

A combination of the ThT assay, spectrofluorometer, and fluorescence microscopy studies revealed that particles induced a slight enhancement in the rate of insulin fibrillation at low particle to protein weight ratios (1:10000 and 1:100). However, once the particle to protein ratio was increased to 1:1, protein fibrillation was accelerated and the nucleation time for the formation of fibrils was significantly reduced. Studies of

protein adsorption on particle surfaces revealed that increasing amount of proteins adsorbed on particle surfaces as the particle to protein ratio was enhanced. In summary, these results reveal that insulin fibrillation is highly influenced by the presence of particles, and fibrillation rate is enhanced due to protein adsorption on particle surfaces; however, particle surface-functional groups do not significantly affect protein fibrillation behavior.

Dedication

This thesis is dedicated to the most influential individuals of my life, my father Mehrab and my husband Sadegh.

Acknowledgments

I would like to take this opportunity to express my gratitude to the following people, without whom I would not have completes my master's degree!

Firstly, I would like to express my appreciation to my academic adviser Dr. Amir M Farnoud for providing guidance, feedback, and encouragement throughout this study. I value all great experiences and research skills that I have gained from working in his lab.

I would also like to thank my committee members, Dr. Douglas Goetz, Dr. Sumit Sharma, and Dr. Justin Holub for helping me with their time, brilliant comments, and collaborative effort during this research. I am also thankful to the Russ College of Engineering and Technology and Department of Chemical and Biomolecular Engineering for giving me this great opportunity to study and peruse my education, and to Tomas Riggs for always being there to facilitate and help with my questions.

Finally, I would like to thank my husband Sadegh for all his loving support and patience he has shown me through this research.

Table of Contents

Page

List of Tables

Page

List of Figures

Page

1. Introduction

1.1 Insulin

Insulin is a hormone that is involved in regulation of blood glucose in the body. Insulin is secreted by beta cells of the pancreatic islands and plays an important role in metabolism of carbohydrates, fats, and proteins [2]. When blood glucose rises above the normal level (5 mM) (hyperglycemia), the beta cells begin producing insulin and release this hormone into the blood stream. Binding to special receptor proteins on the membrane of liver cells, known as the insulin receptors, initiates a signal transduction pathway in the cell leading to the storage of the excess glucose in the liver, muscles, and fat cells as glycogen [3]. This process, called glycogenesis, allows liver cells to maintain the blood glucose level by uptaking excess glucose molecules.

Insulin is composed of 51 amino acids consisting two polypeptide chains: A and B, with 21 and 30 amino acid residues, respectively. In the A-chain, a disulfide bond connects two cysteine amino acids (A6 and A11). A-chain itself is linked to the B-chain by two inter-chain disulfide bonds. The amino acids linked by disulfide bonds are A7–B7 and A20–B19 [4]. These three covalent disulfide bonds endue insulin protein with stability. Amino acid residues also interact together via other interactions such as hydrogen bonds, ionic bonds, and hydrophobic interactions. As a result, the protein will fold into its biologically functional form. Seven amino acid residues in insulin structure can obtain positive charge and ten amino acids are capable of attaining negative charge. Therefore, based on these amino acids' pKa, the net charge of insulin molecule is

negative, zero, and positive at pH of 7, 5.3-5.4, and 2, respectively [2]. Insulin is mainly in the form of a hexamer and monomer in neutral pH and acidic conditions, respectively; however, it can also be found in the form of a tetramer. For instance, at natural pH in presence of zinc, insulin is hexametric or in 20 mM HCl (pH 2.0) is in the form of dimer [5].

Figure 1

Insulin protein structure showing interaction and bonds between amino acids [6].

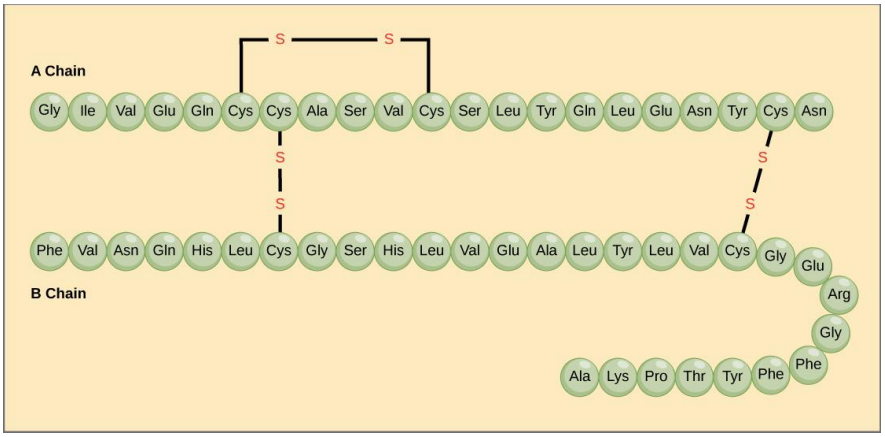

1.2 Protein Fibrillation

Amino acid chains fold and form a native three-dimensional structure. This conformation causes the protein to be biologically functional. Under certain conditions, such as mutations, co-solvents, acidic environment, and high temperature, the three-dimensional structure of proteins will change leading to proteins denaturation [7]. These

misfolded polypeptide chains tend to form β-sheet structures [8]. Many copies of misfolded proteins then stick together and form fibrillary aggregates [9]. These aggregates of protein, called amyloid, are rich in β-sheet structures [10], [11]. Since amyloids are proteins that have lost their physiological functions and have formed aggregates, they can disrupt the normal function of nearby tissues and organs [11]. Amyloids have been associated with more than 20 human diseases, generally classified as amyloidosis, such as Creutzfeldt–Jakob disease, Alzheimer's disease, Parkinson's disease, amyloidosis, prion disease and a wide range of other disorders[12], [13]. In case of human insulinoma, as well as in pancreatic tumors, aggregates and amyloid fibrils have been found and reported [14], [15]. Protein aggregation phenomena is also problematic during the production and purification of protein-based drugs such as insulin that are to be maintained stable at low pH and is one of the major issues in protein production, purification, and storage [16].

1.3 Insulin Fibrillation

Insulin amyloid-like fibrils can pose a variety of problems in its biomedical and biotechnological applications, especially in insulin pumps [17]. Recent studies show the occurrence of insulin amyloids in clinical situations is increasing [18], [19]. Insulin fibril deposition at the site of injection after repeated injection is a problem in patients with type II diabetes [18], [20]. Patients typically receive two to four injections of insulin per day, totaling one to two units of insulin (each unit=0.0347 mg of insulin) for every kilogram of body weight. The fibrils also have been observed in normal aging [21].

During fibrillation process, the quantity of alpha-helix structures in insulin molecule decreases and the amount of beta-sheet structures increases. Thus, insulin fibrils have high content of beta-sheet structure [22]. The process in which misfolded proteins aggregate and form fibrils is called protein fibrillation. Using electron micrographs, insulin fibrils have been shown to have variable lengths with a width of 17–20 nm and a height of 8–10 nm [23], [24].

It has been proposed that insulin fibrillation involves dissociation of the native protein into monomers, which then form oligomers. Protofibrils are formed from the attachment of oligomers, which have a high propensity to join each other and form fibrils [25]. Protein fibril formation consists of three phases (Figure 2). Phase one: a nucleation phase/lag phase, in which monomers undergo conformational changes leading to protein misfolding and formation of nuclei, phase two: elongation phase, in which the nuclei rapidly grow by further addition of monomers and oligomer protofibrils and phase three: in which protofibrils become mature, thick and long fibrils. This phase is called saturation phase. In contrast to the nucleation phase, which is the most time-consuming phase, elongation phase proceeds quickly [10], [26], [27]. Formation of oligomers occurs at the lag phase in spherical bead-like shapes with a width of ~60 nm. Protofibrils formed at the end of elongation have been shown to be single-stranded and non-branched fibrils with ~100 nm thickness whereas mature fibrils at saturation phase are long and branched having thickness of 150 nm [28], [29].

Figure 2

Nucleation-dependent fibril formation process [30].

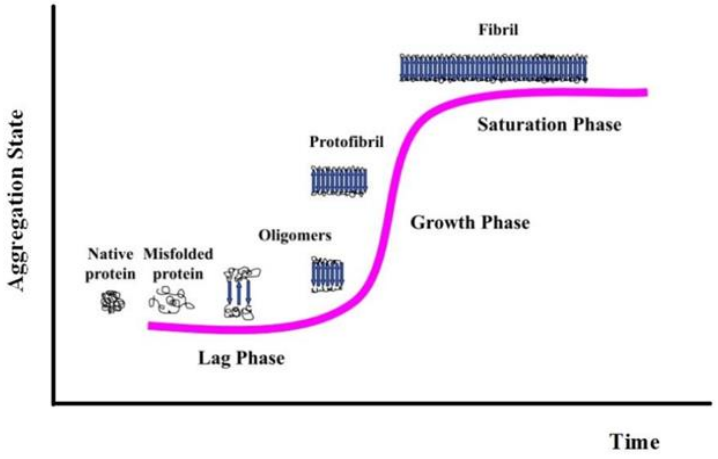

1.4 Nanoparticle-Protein Interactions

Nanoparticles (NPs) are materials that have at least one dimension less than 100 nm. Due to their large surface-to-volume ratio, NPs show significant adsorptive behavior and are suitable for binding with drugs, probes, chemical compounds, and proteins. Nanoparticles can be produced with various physical and chemical properties such as size, charge, surface chemistry and components making them potential candidates to be studied for their effects on protein fibrillation. Nanoparticles have been reported to alter the fibrillation of proteins [31]–[35]. Lynch et al. proposed that nanoparticles modulate protein fibrillation due to their small size and high surface area-to-volume ratio [36]. Proteins either attach to the surface of NPs by covalent bonds or get immobilized onto NPs' surfaces by physical adsorption [37]. By affecting mainly the nucleation phase of

fibrillation, particles can enhance or retard fibrillation process [38]. In fact, nanoparticle surfaces can act as nucleation sites for protein association, which induces significant changes in protein structure and the rate of protein fibrillation [39]–[41].

Figure 3

Nanoparticles and proteins interaction [42].

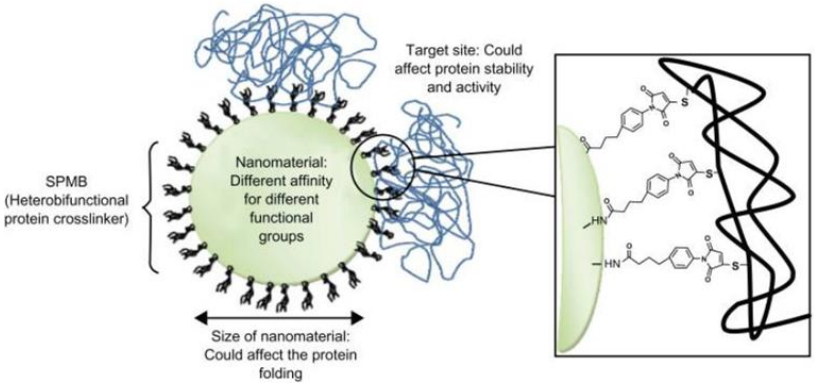

The majority of the studies on nanoparticle-induced alterations in insulin fibrillation have used the thioflavin T (ThT) assay to measure the rate of fibrillation. ThT is a widely used fluorescent dye to visualize and quantify protein fibrils. ThT molecules can bind to β-sheet structures in amyloid fibrils. Upon binding to β-sheet structures in amyloid fibrils the fluorescence emission of the dye will increase [43], [44] (Figure 4).

Figure 4

Thioflavin T (ThT) assay [45].

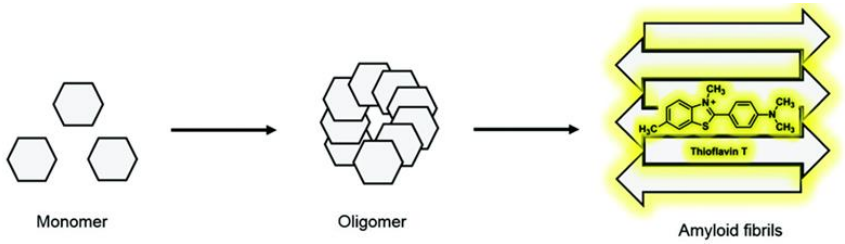

Amyloid beta (Aβ) fibrillation is associated with Alzheimer's disease as it is the main component of the amyloid plaques found in the brains of Alzheimer patients [46]. Hence, understanding the underlying mechanism of Aβ fibrillation and aggregation is critical to diagnosis and prevention Alzheimer's disease. Many studies have evaluated the effects of nanoparticles on Aβ fibrillation. Several studies have reported that nanoparticles can enhance Aβ fibrillation rate. For instance, Wu et al. proposed that the interaction between Aβ and nanoparticles may contribute to Alzheimer's disease [47]. They treated Aβ with titanium dioxide (TiO_2) and demonstrated that these nanoparticles promote fibrillation. Representing the data that TiO_2 with concentration of 0.1 mg/mL has produced fast fibrillation by shortening the lag time. Wu et al. explain that TiO_2 nanoparticles can promote Aβ fibrillation rate by decreasing the nucleation process, which is the rate-determining step of fibrillation. They also demonstrated that the higher the concentration of concentration of TiO_2, the faster the fibrillation of Aβ will be.

Authors explained that the reason of promoting effect of Aβ fibrillation is due to the ability of TiO_2 nanoparticles to adsorb Aβ on their surface which leads to a local high am Aβ monomer concentration on the surface. This situation can shorten the lag time of nucleation which eventually results in the rate enhancement of Aβ fibrillation.

On the other hand, several studies have reported that some nanoparticles are able to decrease the rate of Aβ fibrillation as a result of protein-nanoparticle interaction. For example, Xiao et at. demonstrated that Aβ fibrillation can be inhibited by N-acetyl-L-cysteine capped quantum dots (NAC-QDs). They proposed these particles (with a typical core size of 2–10 nm) inhibit fibrillation by diminishing the nucleation and elongation processes. The reason for inhibition of fibrillation was proposed to be hydrogen bonding between NAC-QDs and amyloid fibrils, which blocks the active elongation sites on the fibrils [33]. Thakur et al. have also reported that dihydrolipoic acid (DHLA)-capped CdSe/ZnS quantum dots (QDs) of approximately 2.5 nm in size can reduce the fibrillation of a Aβ [48]. Less fibril formation was detected as a result of the interaction of DHLA-capped QDs to Aβ. The morphology of amyloid β fibrils mixed or conjugated to the QDs was significantly changed very much evidenced by transmission electron microscopy (TEM) and atomic force microscopy (AFM) images.

The effect of hydrophobic Teflon nanoparticles on the conformation of the Aβ has been investigated by Giacomelli et al [49]. They demonstrated that increased Aβ absorption on the surface of Teflon particles results in enhancement of the β-sheet conformation in the protein [49]. Cadmium telluride nanoparticles (CdTe NPs) were

selected by Yoo et al. to investigate their effect on the fibrillation of amyloid beta. It was shown that CdTe nanoparticles can inhibit Aβ fibrillation by extending the lag phase in a dose-dependent manner. Representing data from SOFAST-HMQC NMR spectra, atomic force microscopy (AFM), transmission electron microscopy (TEM), and fluorescence spectroscopy data, author suggested that the inhibition because of the binding of CdTe NPs to Aβ oligomers rather than individual monomers. As a result of particles and oligomers interactions, oligomeric bands became noticeably weaker and fibrillation was decreased [32].

Moore et al. have demonstrated that both nanoparticles' diameter and surface chemistry contribute to the formation of aggregations and fibrils. Applying gold nanospheres, the effect of different surface coatings and diameters on Aβ fibrillation was investigated. Citrate- PAH-coated NPs with 8 nm and 18 nm in diameter inhibited Aβ aggregation significantly although smaller anionic NPs were stronger inhibitors. Both nanoparticle diameter and surface chemistry were reported to regulate the amount of aggregation, whereas NP electric charge altered the morphology of aggregations [50]. They suggested that these findings can give us an insight into designing engineered nanoparticles being effective for Alzheimer's disease therapeutics. Another study by Elbassal et al. have applied gold nanoparticles (AuNPs) to study the formation of Aβ amyloid fibrils and oligomers. They demonstrated that as the quantity of Aβ40 amyloids increased, the intensity of the surface plasmon resonance (SPR) absorption band of the AuNPs also increased [51].

Mechanistic understanding of the Aβ fibrillation process can be applied for development of therapeutic strategies in amyloid-related diseases. In an effort to study the Aβ fibrillation mechanism, Skaat et al. designed two types of engineered biocompatible nanoparticles containing different hydrophobic dipeptides in the polymer side chains. One of those polymer nanoparticles was composed of monomers N-acryloyl-L-phenylalanyl-L-phenylalanine methyl ester (A-FF-ME) with size of 57 ± 6 nm. The other polymer was composed of L-alanyl-L-alanine (AA) dipeptide (A-AA-ME) in the polymer side groups. The dipeptide residues were designed such that they are similar to the hydrophobic core sequence of amyloid beta. Applying polyA-FF-ME nanoparticles on Aβ 40, a significant inhibition effect was recorded and transition of amyloid beta sheet secondary structure from random coil to beta-sheets was diminished as a result of protein-nanoparticle interaction. On the other hand, poly (A-AA-ME) nanoparticles accelerated the Aβ (40) fibrillation rate. Authors concluded that nanoparticles with different surface chemistry can have different effects on insulin fibrillation rate [52].

Nanoparticles can induce changes in protein structure, which results in conformations favoring fibrillation [53]. Superparamagnetic iron oxide nanoparticles (SPIONs) are known to be biocompatible so they have potential to be used in the diagnosis and treatment of various brain diseases such as Alzheimer's disease. Prior to clinical application of SPIONs, this is crucial to understand how these nanoparticles interact with Aβ proteins. Subsequently, Mahmoudi et al. studied the interactions of SPIONs with Aβ and demonstrated a reduction in Aβ fibrillation rate in the presence of

SPIONs. Proteins can form nuclei on the surface of nanoparticles, resulting in deceleration of fibrillation. Cabalerio-Lago et al. analyzed the interaction of Aβ protein with 57 nm amino-modified polystyrene nanoparticles. The results highlighted the importance of particles' surface area and the ratio between Aβ protein and nanoparticle concentration. Depending on the concentration ratio between the protein and the particles, the kinetic for Aβ fibrillation can alter from acceleration of the fibrillation process by lowering the lag phase at low particle concentration in solution to inhibition of the fibrillation at high particle concentration. Since the inhibition effect follows a dose-dependent fashion (the lag time decreases as the nanoparticle concentration is increased), they proposed the nucleation at the particle surface can be the reason of promoted fibrillation [54].

Although Aβ fibrillation has been a topic of intense research, fibrillation of insulin is also a problematic issue in pharmaceutical industry for insulin production and purification. On the other hand, insulin fibrillation has been reported to be related to diabetes mellitus [55]. Hence, a few studies have been performed to investigate the effects of nanoparticles on insulin fibrillation. For instance, Skaat et al. [56] have studied the effect of maghemite magnetic nanoparticles Fe_2O_3 of 15.0 ± 2.1 nm on insulin fibrillation and took advantage of the magnetic properties of these nanoparticles to separate fibrils in an aqueous solution. In that study, human insulin amyloid fibrils were formed by incubating the monomeric insulin dissolved in aqueous solution at 65 °C (pH 1.6). After fibril formation, maghemite nanoparticles were added and kinetics of insulin

fibrillation in the absence and the presence of the particles were measured. A similar behavior was observed showing no effect of nanoparticles on insulin fibrillation. The authors demonstrated that maghemite nanoparticles attach to amyloid fibers and can be extracted from the aqueous phase by applying a magnetic field [56]. Using this selective extraction method, they hypothesized that this method can be applicable for the removal of other amyloidogenic proteins leading to neurodegenerative diseases like Alzheimer's, Parkinson's, Huntington's, mad cow, and prion diseases from their continuous phase (e.g. milk, blood, neurological fluid).

Quantum dots (QDs) have great potential to be used for diagnostic and therapeutic studies because they have broad absorption spectra, narrow emission spectra, and high photostability [57]. Sukhanova et al. have reported the result of their study about the effect of CdSe/ZnS QDs coated with a modified Polyethylene glycol (PEG)-OH polymer (PEGylated CdSe/ZnS QDs) on the fibrillation of insulin. Using techniques such as circular dichroism (CD), Thioflavin T (ThT) fluorescence assay, dynamic light scattering (DLS), different stages of the fibrillation process was analyzed. They recorded a significant increase in insulin fibrillation rate after mixing those nanoparticles with insulin. It was concluded that PEGylated CdSe/ZnS QDs considerably enhance the formation of amyloid-like fibrils of human insulin under physiological conditions. Hosseinzadeh et al. investigated the effect of ZnO QDs on insulin fibrillation. The results from CD spectroscopy shows a decrease in alpha helices structure of insulin in the presence of ZnO QDs. Thermal aggregation study (a useful method showing the

resistance of proteins to the thermal denaturation) of protein at wavelength of 360 nm is also illustrated insulin fast fibrillation as a result of protein-nanoparticle interaction [58]. Yousefi et al. studied the fibrillation of insulin in the presence of homocysteine thiolactone (HCTL) and reported faster fibrillation as a result of insulin-nanoparticles interactions and a transition from α-helix into predominantly β-sheet structures [59].

In contrast to the studies described above, which reported acceleratory effect of nanoparticles on insulin fibrillation, some other studies have described inhibitory effect by nanoparticles on insulin fibrillation. For example, Li et al. reported that Carbon Dot (C-Dot) nanoparticles inhibit insulin fibrillation [34]. C-Dots were mixed with human insulin to study their effect on insulin fibrillation. Using Thioflavin T (ThT) assay, the kinetics of insulin fibrillation and its three-stages (lag phase, elongation phase, and saturation phase) were characterized by the ThT fluorescence, considering this fact that as amount of aggregation and fibrils increases, ThT fluorescence intensity is enhanced consequently [60], [61]. C-Dots were very inhibitive to insulin fibrillation even at low concentrations. For example, 40 μg/mL of C-Dots prevented the fibrillation of 0.2 mg/mL of insulin for 5 days under 65 °C, whereas insulin fibrillation happened in 3 hours under the same conditions in the absence of nanoparticles. Inhibition was suggested to be due to the interactions between C-Dots and insulin species during lag time and before elongation phase. Another study conducted by Lu et al. studied the effect of core-shell nanoparticles, consisting of Fe_2O_3 (maghemite) core, coated with carboxymethyl-dextran (CM-Dex NPs), on insulin fibrillation. The authors reported inhibitory effects on insulin

fibrillation by nanoparticles and suggested that the extent of inhibitory activity of nanoparticles on human insulin fibrillation is associated with the physio-chemical properties of nanoparticles. Therefore, they proposed that nanoparticles with an appropriate surface modification can be utilized to prevent fibrillation of proteins [60]. Another study performed by Zhou et al. demonstrated that pentapeptide Phynilalanine-Valine-Proline-Argenine-Lysine (FVPRK) homology to the C-terminal of the insulin receptor α-CT can interact with insulin and create a supramolecular assembled nanoparticle. As a result of pentapeptide and insulin interaction, insulin fibrillation rate was reported to be decreased. The results suggest that supramolecular nanoparticles consisting of insulin and pentapeptide have the potential to be used for insulin therapy [61].

Although there have been some studies on the role of nanoparticles on kinetics of insulin fibrillation, the mechanisms by which nanoparticles affect insulin fibrillation is still not well-understood. This contributes to a lack of understanding of how and why nanoparticles accelerate or inhibit insulin fibrillation process. Understanding of how insulin fibrillation might be affected by nanoparticles could result in having a mechanistic perception of interaction between engineered nanoparticles and insulin. This might lead to the development of strategies to detect, prevent, and treat insulin fibril toxicity in patients with type II diabetes and other protein-misfolding diseases such as Alzheimer's disease and Parkinson's disease. In addition, having this knowledge could facilitate the development of guidelines on the health risks of engineered nanomaterials. This research

pursues two main aims: 1. Investigation of the effect of nanoparticle physicochemical properties on insulin fibrillation and 2. Investigation of the mechanisms by which nanoparticle physicochemical properties affect insulin fibrillation. Polystyrene nanoparticles provide a model for this research as they are commercially available with various surface chemistries. Using 200 nm polystyrene particles modified with amine or sulfate groups offers insight into how changes in nanoparticle surface chemistry affect fibrillation process. Based on previous studies, our hypothesis is that nanoparticle physicochemical properties regulate insulin fibrillation rate because of protein-nanoparticle interactions.

2. Materials and Methods

2.1 Commercial Reagents

Sulfate-modified (lot: 1719264) and amine-modified polystyrene particles (lot: 1843344), both with a nominal diameter of 200 nm, were purchased from ThermoFisher (Waltham, MA). Acetone and ethanol 200 proof used for cleaning purposes in the experiments were purchased from Fisher Scientific (Hampton, NH) and Decon Labs Inc. (King of Prussia, PA), respectively. Purified water was obtained from an ELGA PURELAB Classic water purifier (High Wycombe, UK). Recombinant human insulin was purchased from Sigma-Aldrich (St. Louis, MO) and MP Biomedicals, LLC (Solon, OH). Thioflavin T (ThT, lot: M6490) was purchased from MP Biomedicals LLC. (Santa Ana, CA). Sodium chloride, hydrochloric acid, and BCA assay kit were purchased from Fisher Scientific. Nucleopore (Polycarbonate) membrane 100 nm Lot: 7002427, filter supports, and 1000 µL syringe were purchased from Avanti Polar Lipids (Alabaster, AL).

2.2 Characterizing Insulin Fibrillation Kinetics

2.2.1. Preparing Insulin Solution with Fibril Inducing Conditions

Recombinant human insulin purchased from Sigma-Aldrich (St. Louis, MO) and MP Biomedicals, LLC (Solon, OH) was dissolved in hydrochloric acid aqueous solution containing 0.1 M NaCl at pH=1.6 to obtain 1 mg/mL insulin stock solution. The solution was diluted by hydrochloric solution (pH 1.6) to make 0.2 mg/ml insulin solution. The insulin solution was then incubated at 65 ^{o}C in an oven without shaking.

2.2.2. Monitoring Insulin Fibrillation by Using the ThT Assay

ThT with a concentration of 40 μM solution was used to evaluate the kinetics of insulin fibrillation formation. A 40 μM ThT solution was made by dissolving 1.275 mg of ThT in 100 mL solution of acidic NaCl. The mixture was then vortex-mixed for 5 minutes and covered in aluminum foil to avoid photobleaching. Every 30 minutes, aliquots of insulin solution (1 mL) were taken and mixed with 40 μM ThT solution (1 ml). The fluorescence intensity of the mixture was measured using a Fluorolog-3 spectrofluorometer (Horiba Scientific, Edison, NJ) at excitation and emission of 440 and 485 nm with excitation and emission slit widths of 2 and 2 nm, respectively. This method was used to monitor fibrillation as a function of time.

2.2.3. Nanoparticle Characterization

Particle size and zeta potential was measured using a ZetaSizer instrument (ZetaSizer Nano ZS, Malvern Pananalytical, Worcestershire, UK). Particle size was measured using dynamic light scattering (DLS). DLS is based on particle Brownian motion in liquid. Small particles move or diffuse more quickly in a liquid than larger particles, which can be used to relate particle diffusion rate to particle size (Figure 5).

Figure 5

Measuring the size of the particle by ZetaSizer [62].

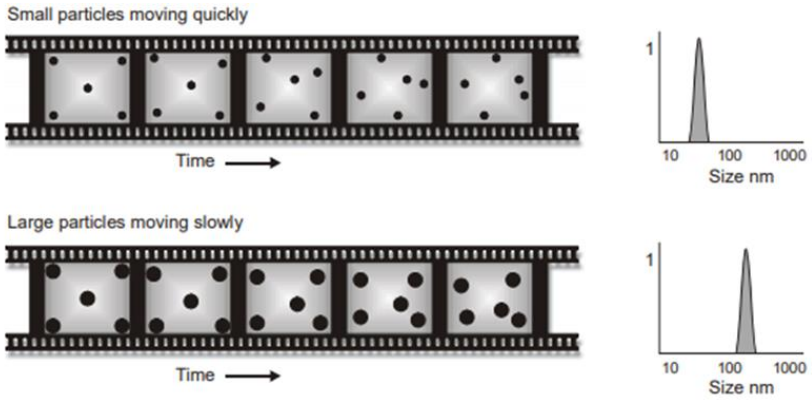

Using DLS in combination with an applied electric field which is called electrophoresis, ZetaSizer can measure particles' zeta potential. Technically speaking, once colloidal suspensions of particles are placed in an electric field, any charged particles or molecules will migrate toward oppositely charged electrode. Based on the time that particles need to pass a known distance, the electrophoretic mobility of particles can be calculated (the velocity of particles depends on their charge), which can in turn be used to estimate the particle zeta potential using established theories.

In order to characterize the size and zeta potential of nanoparticles, and zeta potential nanoparticles were dispersed in HCl aqueous solution containing 0.1 M NaCl (pH 1.6) to obtain the concentration of 0.01 mg/mL. The samples were vortexed for 5 minutes, sonicated for 15 minutes, and then poured into a disposable cuvette with a 1-cm

light path and illuminated with a standard laser with at wavelength of 633 nm at temp 25 ◦C using ZetaSizer.

2.2.4. Treating Insulin Solution with Nanoparticles

Particles with concentrations of 0.02, 2, or 200 μg/mL were suspended into deionized (DI) water. Particle suspensions were then vortex-mixed and sonicated twice for 5 and 15 minutes to ensure lack of aggregates. Particle size and charge was evaluated using dynamic light scattering and laser Doppler anemometry using a particle size analyzer (ZetaSizer Nano ZS, Malvern Pananalytical, Worcestershire, UK). Recombinant human insulin was dissolved in 0.1 M NaCl and adjusted to a final pH of 1.6 using hydrochloric acid, at a concentration of 0.2 mg/ml. Then 0.02, 2, or 200 μg/mL of particles, corresponding to protein to particle ratios of 10000:1, 100:1, and 1:1, were added to the protein solution prior to the start of the fibrillation experiment. The insulin-nanoparticle suspensions were incubated at 65 °C for 5 hours. The fluorescent probe, ThT, was used to evaluate the kinetics of insulin fibrillation in presence of nanoparticles. Every 30 minutes, 1 mL aliquots were taken from the insulin solution and mixed with 1 mL of 40 μM ThT solution. The fluorescence intensity of ThT in the resulting mixture was measured using a spectrofluorometer at an excitation wavelength of 440 nm and emission wavelength of 485 nm with slit width of 2 nm for both excitation and emission.

2.2.5. Fluorescence Microscopy

The presence of fibrils was visually inspected using digital inverted fluorescence microscope (EVOS fl, AMG, Mill Creek, WA). For these experiments, insulin solution, incubated at 65 ◦C and pH of 1.6 with or without particles, was aliquoted at 0, 1.5, 3, 4, and 4.5 hours after incubation and mixed with a 40 μM ThT solution. The resulting mixture (20 μL) was imaged using fluorescence microscopy with 20X magnification.

2.2.6. Atomic Force Microscopy (AFM)

To prepare fibrils for imaging with Asylum Research MFP-3DTM AFM (Santa Barbara, CA), insulin samples with concentration of 0.2 mg/mL were first diluted 1:100 with deionized water and then an aliquot of 20 μL drop-coated on glass slides. After being dried for 34 hours at room temperature, the samples were studied with AFM using tapping mode technique Protein adsorption on particle surfaces

For this experiment, recombinant insulin was dissolved in in 0.1 M NaCl (pH 1.6) with a concentration of 0.2 mg/mL. Next, amine and sulfate-modified nanoparticles with three concentrations of 0.2, 0.002, 0.00002 mg/mL were prepared, vortex mixed, and sonicated for 15 minutes. Subsequently, amine and sulfate-modified nanoparticles with insulin protein ratios of 1:1, 1:100 and 1:10000 were incorporated into six insulin solution samples with a concentration of 0.2 mg. Insulin in the absence of nanoparticles was used as the control. After 1 hour of incubation at 65 ^{o}C, which is less than the time expected to result in protein fibrillation, each incubated insulin-nanoparticle sample plus control (i.e. insulin without nanoparticles) were filtered using an extruder containing 100

nm polycarbonate membrane filter to separate free insulin proteins that have not been adsorbed on the surface of nanoparticles. Knowing the initial concentration of insulin protein (0.2 mg) and measuring the concentration of filtered insulin-nanoparticle samples, using the BCA assay, allowed for estimation of the amount of insulin on the surface of nanoparticles. Following the same procedure, concentration of insulin proteins on the surface of particles after 2 hours was also calculated.

Preparation of Standards and Working Reagent for Bicinchoninic Acid Assay (BCA).

Using Table 1 as a guide, a set of diluted albumin standards were prepared. Each 1mL ampule of 2 mg/mL albumin standard is enough to prepare a set of diluted standards for three replicates of each diluted standard. Contents of one albumin standard ampule was diluted into nine clean vials marked as A to I. DI water was used for dilution of albumin standard.

Table 1

Preparation of diluted bovine serum albumin (BSA) standards.

Vial	Volume of Dilute (µL)	Volume and Sorce of BCA (µL)	Final BCA Concentration (µg/mL)_
A	0	300 of Stock	2000
B	125	375 of Stock	1500
C	325	325 of Stock	1000
D	175	175 of vial B dilution	750
E	325	175 of vial C dilution	500
F	325	175 of vial E dilution	250
G	325	175 of vial F dilution	125
H	400	175 of vial G dilution	25
I	400	0	0 = Blank

Using the following formula to determine the total volume of BCA Working Reagent (WR) required: (# standards + # unknowns) × (# replicates) × (volume of WR per sample) = total volume WR required. For each sample in the microplate procedure only 200 µl of WR reagent was required. WR was prepared by mixing 50 parts of BCA Reagent A (containing sodium carbonate, sodium bicarbonate, bicinchoninic acid and sodium tartrate in 0.1 M sodium hydroxide) with 1 part of BCA Reagent B (containing 4% cupric sulfate). The ratio of reagent A to reagent B must be 50:1. When Reagent B was first added to Reagent A, turbidity was observed that quickly disappeared upon

mixing to yield a clear, green WR. Sufficient volume of WR was prepared based on the number of samples to be assayed. The WR was stable for several days when stored in a closed container at room temperature (RT).

Microplate Procedure for BCA Assay.

The BCA standards were made following the kit instructions. Three replicates of 25µL from each standard or unknown sample replicate was pipette into a microplate well. The procedure was started with sample I, which had the lowest concentration, and continued to sample A, with the highest concentration, so that there was no need to change pipet tips. Then, 200 µL of the WR was added to each well of a 96-Well plat and mixed thoroughly by moving the plate on a flat surface for 30 seconds. The plate was covered with aluminum foil and incubator at 37 °C for 30 minutes. After cooling the plate in room temperature for 10 minutes, the absorbance of samples was measured at 562 nm on a plate reader.

The principle of this method is that proteins can reduce Cu^{+2} in to Cu^{+1} in an alkaline environment and result in a purple color. Therefore, the darker the purple color is, the more concentrated the protein will be. The reduction of copper is mainly because of four amino acid residues such as cysteine or cystine, tyrosine, and tryptophan that are present in protein molecules. This complex of protein and WR shows a strong absorbance at 562 nm that is almost linear with increasing protein concentrations for a range of 20-2000 µg/ml [63].

2.2.7. Circular Dichroism Spectroscopy

Insulin was dissolved in hydrochloric acid aqueous solution (pH 1.6) containing 0.1 m sodium chloride (NaCl), with concentration of 0.2 mg/ml, with or without nanoparticles. Only a protein to particle weight ratio of 1:1 was used for these studies. Therefore, two samples were prepared. One sample as a control without nanoparticles and the other one was treated with nanoparticles with mass ratio of 1:1. They were then incubated at 65 °C for t=1, 3, 4 hours. At each time point, 125 μl of samples at each time point (t=1, 3, 4 hours) were diluted with acidic NaCl, containing 40 μM of ThT to reach 250 μl with concentration of 0.1 mg/ml. Diluted samples were then poured into a cuvette with a 1-mm light path to record CD spectra. In this study, conformational changes of insulin during fibrillation, in the presence and absence of particles, was examined using a JASCO J-810 spectropolarimeter (Easton, MD) with following settings: temperature 25 °C, wavelength from 190 to 260 nm, band width 10 nm, resolution 0.1, speed 20 with sensitivity of 20 mdeg, and response 1 sec. Initially, CD spectra of a blank sample without any protein or particles, only containing 0.1m NaCl and HCl with pH 1.6 was recorded at wavelength between 190 and 260. The spectra of blank then subtracted from the spectra of all experimental samples.

3. Results

3.1 Kinetic of Insulin Fibrillation

Insulin fibrillation kinetics in the absence of nanoparticles was characterized to ensure that the fibrillation profile is in accordance with the literature. Using the ThT assay, kinetics of insulin fibrillation under denaturing condition (pH 1.6 and 65 °C) was monitored. For this experiment, the insulin solution with concentration of 0.2 mg/mL was incubated at 65 ^{o}C for 7.5 to 8 hours and every 30 minutes fluorescence intensity of ThT was detected. Using a sensitive spectrofluorometer, the fluorescence intensity of ThT and subsequently the amount of fibrils formed were measured. This assay resulted in a fibrillation profile that was in good agreement with the literature [34] as shown in Figure 6.

Figure 6

Kinetics of fibrillation for an insulin solution (0.2 mg/ml) in HCl at 65 °C and comparison with the literature. The graph indicates the fluorescence intensity of ThT at excitation and emission of 440 and 485 nm respectively with slit widths of 1 and 1.6 mm. A) The insulin fibrillation profile generated in the lab and B) fibrillation profile reported in the literature [34].

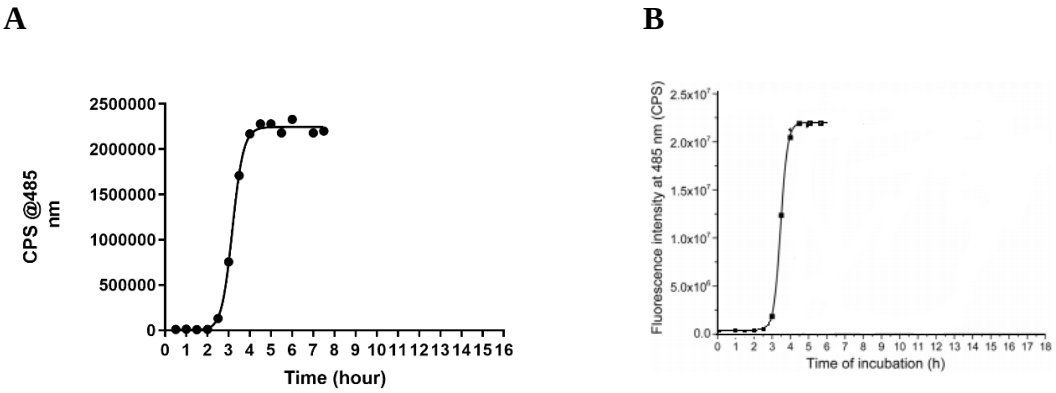

*(Curve fit is sigmoidal 4X, X is a log). Equation: Y=Bottom + (Top-Bottom)/(1+10^((LogEC50-X) * HillSlope))*

Using the ThT assay, three stages can be observed in insulin fibrillation profile: a lag phase, an elongation phase, and a saturation phase. Low fluorescence intensity values are recorded through the lag phase whereas a rapid increase in fluorescence intensity happens during the elongation phase. Eventually, saturation phase begins; during this phase fluorescence intensity of ThT does not change considerably and remains relatively

constant. Various lag times of 1.5, 2, 2.5 hours were also recorded in insulin fibrillation process while the fibrillation profile was the same (Figure 7).

Figure 7

*Kinetics of fibrillation for an insulin solution (0.2 mg/ml) in HCl at 65 °C. The graph indicates the fluorescence intensity of ThT at excitation and emission of 440 and 485 nm respectively with slit widths of 1 and 1.6 mm. In some experiments lag time was measured to be 1.5, 2 and 2.5 hours considering the same experimental condition and the same protocol to prepare insulin and measure the fluorescence intensity. A) Lag time is 1.5 hr, equation: Y=22235 + (2098430-22235)/(1+10^((Log215.8)-X) *1.44)). B) The lag time is 2 hr, equation: Y=18732+ (2171185-18732)/(1+10^((Log446.7)-X) *1.941)). C) Lag time is 2.5 hr, equation: Y=20789 + (2116138-20789)/(1+10^((Log1369-X) *1.77)).*

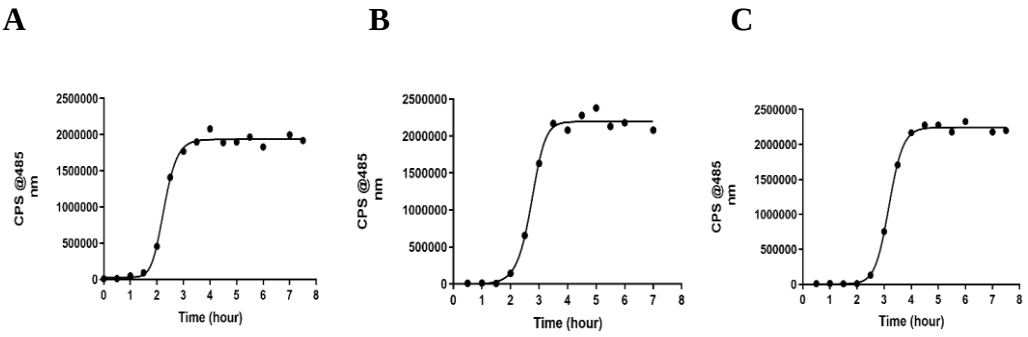

It was previously reported that insulin in acetic acid at pH 1.95 predominantly exists as a monomer whereas at pH 1.85 was found to be in form of dimers [64]. Another study described the role of dimers and monomers in insulin fibrillation. According to the

results, insulin monomers are less stable than other forms such as dimers, tetramers and hexamers [65], [66]. As monomers tend to aggregate, they are known to be fibrillating species [67], [68]. Although all the experiments were performed under the same conditions and with the same protocol, variability in fibrillation lag times could be due to slight differences in the pH of the solution. Since the pH of solution differed between 1.60 to 1.65, this small changes in pH of the solution could be the determining factor for the dominance of insulin monomers over dimers in the solution. As monomers are known to be the fibrillating species, their existence could affect the fibrillation rate and cause different lag times.

3.2 Characterization of Polystyrene Nanoparticles Using ZetaSizer

The zeta potential (surface charge) and size of the sulfate-modified and amine-modified polystyrene nanoparticles were measured using a ZetaSizer instrument. A particle concentration of 0.01 mg/mL was used in these studies. Particle charge and size for sulfate-modified and amine-modified particles were measured to be 3.5 ± 0.4 mV and 241 ± 12 nm, and 21.7 ± 1.3 mV and 223 ± 6 nm, respectively.

3.3 Characterization of Insulin Fibril Structure

ThT is able to bind to structures with high β-sheet content [43], [44] and demonstrates enhanced fluorescence emission, which can be observed by fluorescence microscopy (FM) and measured by spectrofluorometer. The amount of the fluorescent emitted by ThT corresponds to the amount of fibrils formed in a solution. This tendency of ThT to bind to fibrils was used to visually examine fibril formation over time. A, B,

and C in Figure 8 represent the quantity of fibrils at the beginning of lag, elongation, and saturation phases. As shown, at t = 0 no ThT fluorescence can be observed, suggesting a lack of fibrillation. After 2.5 hours, aggregates were formed and at t =4 hours the aggregates were grown to be larger and more visible by FM. The FM images of samples at time 0, 2.5, and 4 hours were in agreement with the results recorded by ThT assay and spectrofluorometer.

Figure 8

Insulin fibrillation as a function of time was characterized by fluorescence microscopy using ThT as the fluorescence probe. (A) Time=0, (B) Time=2.5 hours, and (C) Time=4 hours. All insulin samples were prepared at a pH=1.6 and 65 ^{o}C.

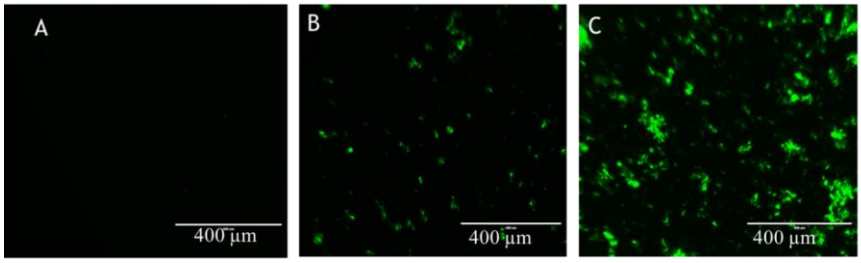

AFM and confocal microscopy were used to visualize the structure of mature fibrils. In comparison with fluorescence microscopy, AFM provides better resolution and does not require the use of a contaminant (ThT). Using AFM, we were able to observe the morphology of insulin fibril (formed after 4 h) in the samples. As shown, long insulin

fibrils appeared in samples after 4 h of incubation at 65 ^{o}C. Fibrils were long, straight, and unbranched, in agreement with literature data (Figure 9).

Fibrils were also examined for their surface charge using a ZetaSizer. At a concentration of 0.1 mg/mL, the fibrils had a charge of -31.5 ± 2.1 mV. Dissolved insulin, free of fibrils, at pH=7 and 1.6 displayed average charge of 26.6 ± 4.7 and 17.4 ± 2.4 mV, respectively.

Figure 9

A) Characterizing insulin fibrils formed after 3.5 hour of incubation 65 °C in acidic environment (pH 1.6). A) Confocal microscopy of mature fibrils B) AFM image of insulin fibrils after 3.5 hour, presented in literature [34]. C) Morphology of insulin fibrils after 4.5 hours of incubation using confocal microscopy.

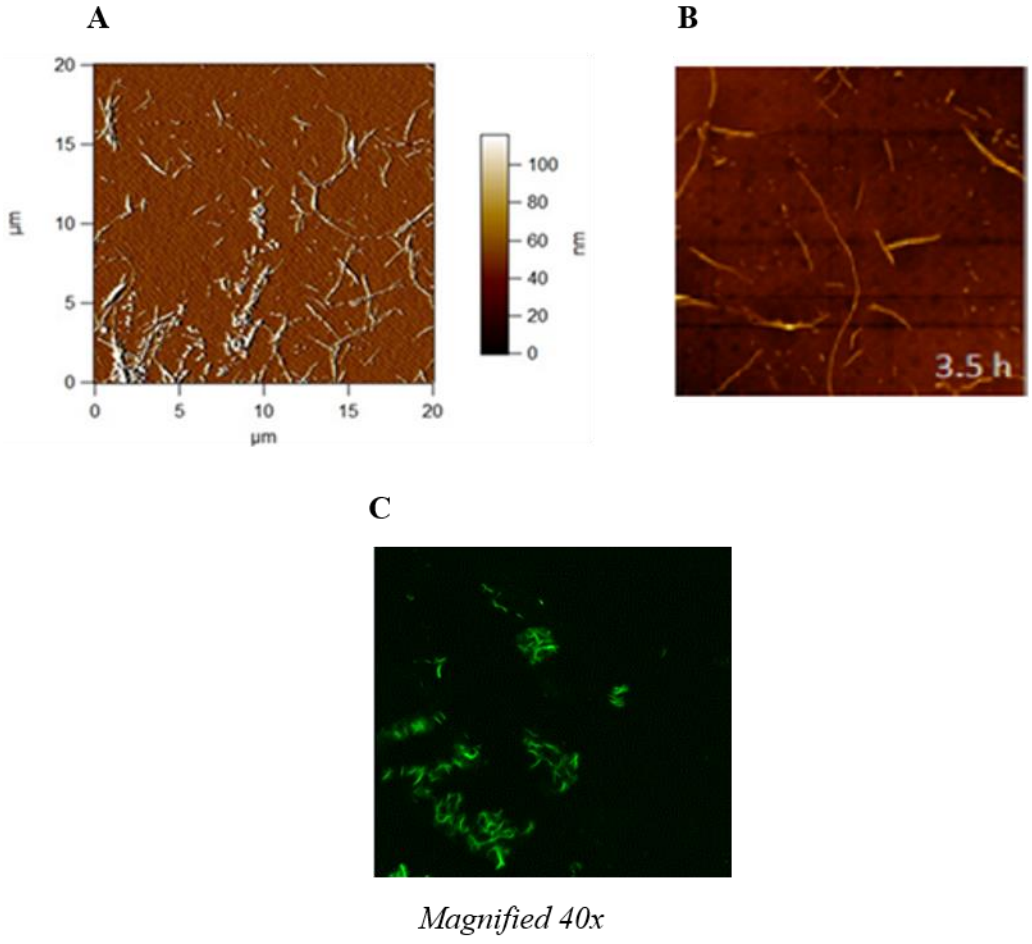

3.4 Nanoparticle Effects on Insulin Fibrillation

The effect of amine and sulfate-modified polystyrene nanoparticles with various concentrations on the kinetics of insulin fibrillation was investigated using the ThT assay and spectrofluorometer. Two samples of insulin with a concentration of 0.2 mg/mL were prepared by dissolving insulin in HCl solution containing 0.1 M NaCl (pH 1.6). One sample served as the control and the other was treated with sulfate-modified particles with a protein to particle weight ratio of 1000:1. Samples were incubated at 65 ^{o}C in an oven for 5 hours. Aliquots of 1 mL were taken out of incubated samples every 30 minutes and were mixed with 1 mL of a 40 μM ThT solution. ThT fluorescence intensity was measured using a Fluorolog-3 spectrofluorometer (Horiba Scientific, Edison, NJ) at excitation and emission of 440 and 485 nm with excitation and emission slit widths of 1 and 1.6 nm, respectively. After six trials the average of fluorescence intensity for each point of time is presented in Figure 10.

Figure 10

*Insulin fibrillation as a function of time and particle concentration after exposure to sulfate-modified polystyrene sub-micron particles (200 nm in diameter). Fibrillation was measured by dissolving 0.2 mg/ml of insulin in HCl solution containing 0.1 M NaCl (pH 1.6) at 65 °C and measuring the fluorescence of the probe ThT at 485 nm. Different weight ratios of proteins to particles (ranging from 10000:1 to 1:1) were used. Error bars show the standard deviation for six independent experiments. * denotes statistical significance compared to control ($p<0.05$).*

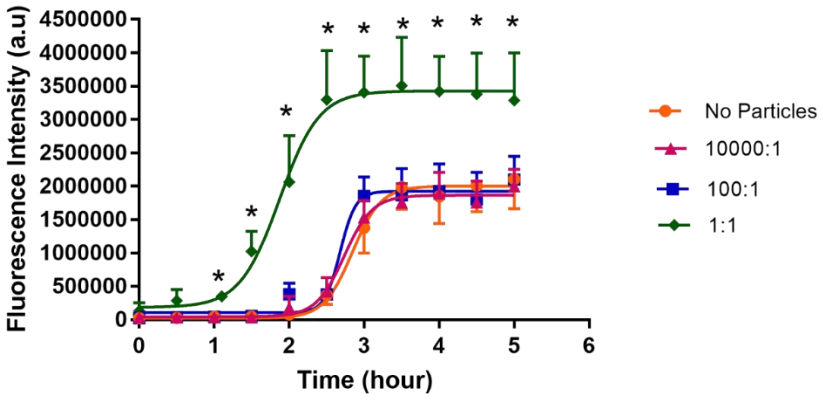

Applying sulfate-modified polystyrene particle with protein-particle weight ratio of 10000:1 did not substantially affect insulin fibrillation in terms of the length of lag time and the amount of fibrils. Increasing the concentration of sulfate-modified particles to protein-particle weight ratio of 100:1 still showed no considerable effect on insulin fibrillation rate. However, at a higher protein-particle weight ratio of 1:1, the lag time

was visibly shortened, and more fluorescence intensity recorded at each point of time, suggesting an increased amount of fibrils (Figure 10).

The effect of amine-modified polystyrene particles on insulin fibrillation was investigated similarly. At a protein to particle weight ratio of 10000:1 amine-modified particles had no significant change on the fibrillation. Similar effects were observed at a protein-particle weight ratio of 100:1 (Figure 11). However, increasing the ratio of protein-amine modified particles to 1:1, a noticeable effect was detected. An acceleration in fibrillation rate was observed as a result of applying amine-modified particles with weight ratio of 1:1. Lag time was shortened and the fluorescence intensity of ThT during both elongation and saturation phase was enhanced significantly. Therefore, acceleration effect of amine-modified nanoparticles happened in two levels of lag time and the amount of fibrils formed.

Figure 11

*Insulin fibrillation as a function of time and particle concentration after exposure to amine-modified polystyrene sub-micron particles (200 nm in diameter). Fibrillation was measured by dissolving 0.2 mg/ml of insulin in HCl solution containing 0.1 M NaCl (pH 1.6) at 65 °C and measuring the fluorescence of the probe ThT at 485 nm. Different weight ratios of proteins to particles (ranging from 10000:1 to 1:1) were used. Error bars show the standard deviation for six independent experiments. * denotes statistical significance compared to control ($p<0.05$).*

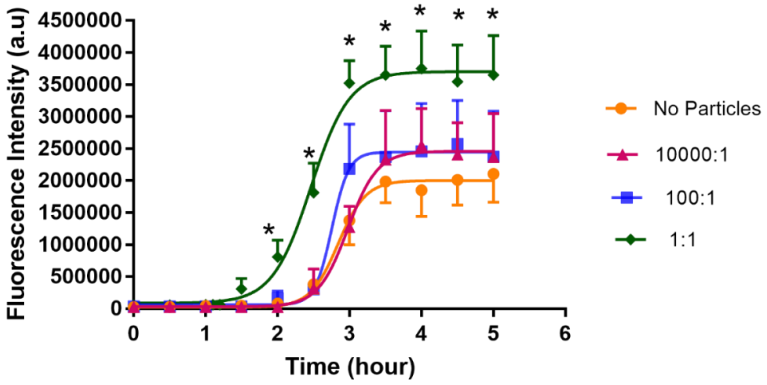

The average of lag time for all sixteen control experiments was calculated to be 2.19 ± 0.46 hours, showing some variability, but a relatively low standard deviation. The average of lag time in the presence of both amine and sulfate-modified nanoparticles with weight ratios of 1:1, 100:1, and 10000:1 was also calculated and compared with control as displayed in Figure 12.

Figure 12

*Changes in the lag phase of protein fibrillation at various protein to particle ratios. Bar graphs represent lag phase of amine-modified vs. sulfate-modified particles with three ratios of 1:1, 100:1, and 10000:1. * denotes statistical significance compared to control ($p<0.05$).*

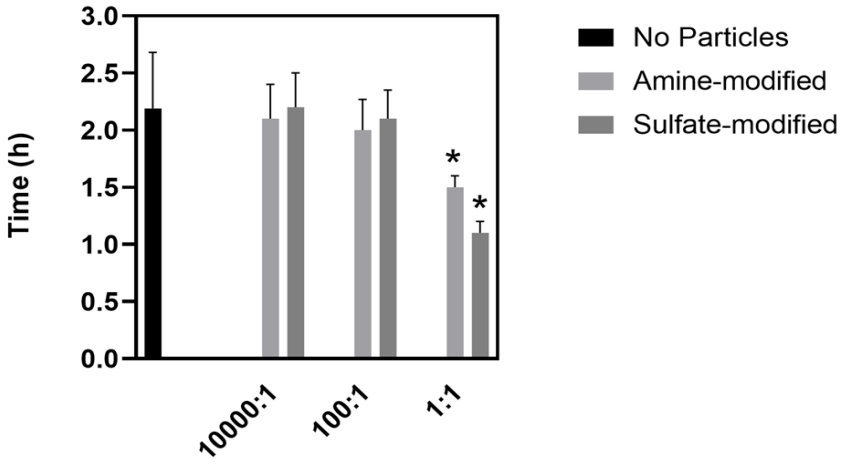

Insulin treated with amine and sulfate-modified particles with weight ratios of 10000:1 and 100:1 (low particle concentration) did not show a significant change in their lag time whereas both amine and sulfate-modified nanoparticle with weight ratio of 1:1 showed significantly decreased lag times. In conclusion, particles significantly affected the kinetics of fibrillation, by affecting the length of the lag phase, which is the first stage of self-assembly of proteins into fibrillar structures.

In addition to affecting the lag phase, the presence of particles also led to a higher fluorescence intensity in the saturation phase (after 4 hours). In saturation phase, protofibrils grow into mature, thick, and long fibrils. Figure 13 shows a comparison between the average of ThT fluorescence intensity during the saturation phase for insulin samples containing amine and sulfate-modified particles with weight ratios of 10000:1, 100:1, 1:1 along with insulin without particles as a control. Applying amine and sulfate-modified particles with weight ratios of 10000:1 and 100:1 have not increased the fluorescence intensity value during saturation phase compared with the value recorded for the control. On the other hand, fluorescence intensity detected from the addition of amine and sulfate-modified particle with weight ratio of 1:1 is significantly higher than control as denoted by a star (*) on top of graph bars.

Figure 13

*Bar graphs represent average of recorded fluorescence intensity from ThT in samples containing no nanoparticle (control) vs. amine-modified and sulfate-modified particles with three ratios of 1:1, 100:1, and 10000:1 during saturation phase (after 4 hours incubation time at 65 °C). * denotes statistical significance compared to control ($p<0.05$).*

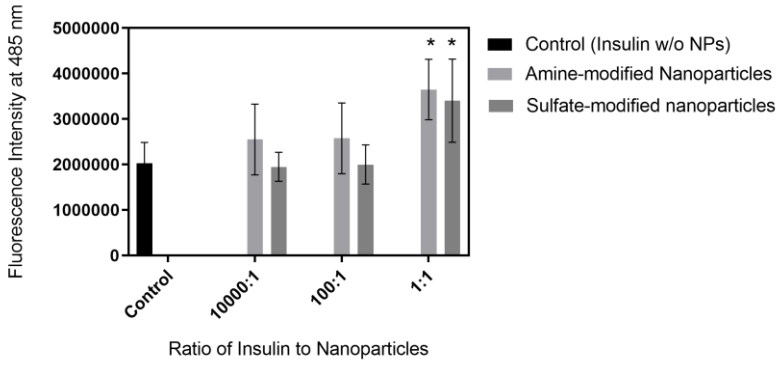

3.5 Acceleration of Insulin Fibrillation Studied by Fluorescence Microscopy

In order to observe the accelerating effect of 1:1 ratio of insulin with amine and sulfate-modified nanoparticles, several images at different time points (0, 1.5, 3, 4.5 hours) were obtained by fluorescence microscopy along with the same time point images of control with no nanoparticles. As shown in Figure 14, fluorescence microscopy images show that in the presence of 1:1 ratio of sulfate and amine-modified nanoparticles with insulin, after 1.5 hours and 3 hours, fibril formation has been accelerated. The results obtained by ThT assay and fluorescent microscopy are in good agreement with each other

and indicated the fibril formation is advanced in the presence of sulfate and amine-modified polystyrene nanoparticles with protein-particle weight ratio of 1:1 (Figure 14).

Figure 14

Comparing fibril formation over various time periods (0, 1.5, 3, and 4.5 h) using fluorescence microscopy. Insulin solution treated with sulfate-modified and amine-modified polystyrene nanoparticles at a protein-particle ratio of 1:1 demonstrated faster fibrillation compared to control. ThT was used as the fluorescent probe. Scale bar in all images is 200 µm.

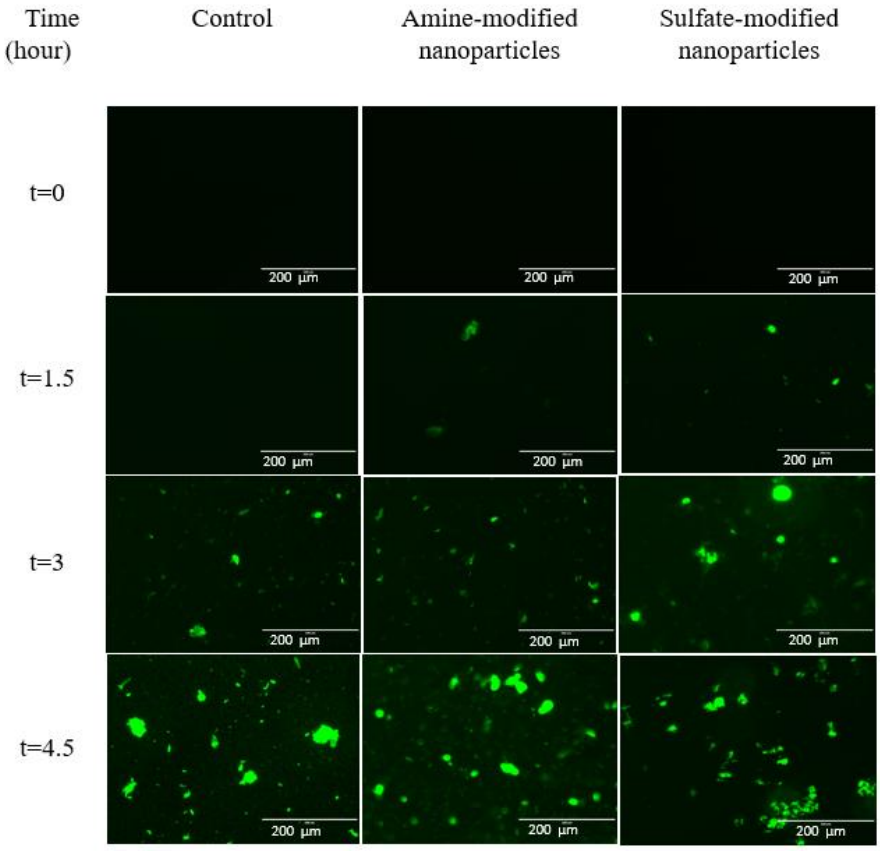

3.6 Measuring Protein Absorption of Nanoparticle Surfaces

Based on the changes observed in fibrillation, it was hypothesized that insulin monomers adsorbed on the surface of nanoparticle (200 nm), forming a nucleus that accelerates fibrillation. Cabaleiro et al. (2008) proposed that a high protein concentration on the surface of nanoparticles could be the reason for enhanced fibril formation by nanoparticles [69]. Although some studies have shown that the fibrillation behavior of proteins changes in the presence of nanoparticles, they have not revealed the mechanism by which nanoparticle physical and chemical properties regulate insulin fibrillation [22], [28], [70]. Insulin monomers attached on the surface of nanoparticles have a higher likelihood of interaction with one another and can form aggregation, which leads to fibril formation. Therefore, by measuring the amount of proteins adsorbed on particle surfaces before the formation of fibrils, we set out to elucidate whether nanoparticles catalyze the aggregation of proteins on their surface and regulate the transformation of protein aggregations into fibrils. Adsorption of insulin on the surface of the particles was examined using the BCA protein assay kit. Measuring the concentration of filtered insulin-nanoparticle samples by applying BCA assay allowed for estimation of the insulin protein concentration on the surface of particles.

Figure 15

Standard curves for bovine serum albumin (BSA) used in the BCA protein assay (n=1) showed a linear relationship between absorbance and protein concentration.

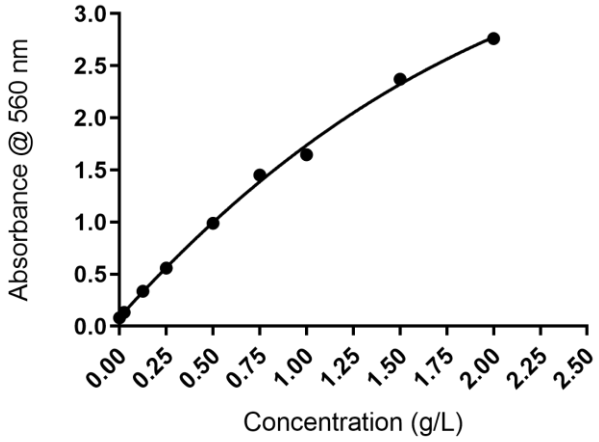

As mentioned earlier, it was hypothesized that adsorption of insulin on the surface of nanoparticles results in accelerated fibrillation. To evaluate this hypothesis, the concentration of insulin on the surface of nanoparticles needed to be quantified. For this purpose, the BCA assay was employed to measure the concentration of insulin after 1 and 2 hours in the absence and in presence of amine-modified and sulfate-modified nanoparticles. To quantify the amount of proteins adsorbed on the surface of nanoparticles, mixtures of insulin with nanoparticles at different ratios (1:1, 100:1, and 10000:1) after 1 or 2 hours of incubation time were filtered through a 100 nm polycarbonate membrane filter. Since this filter size is smaller than the size of the particles, filtration would lead to the entrapment of nanoparticles while free insulin

monomers could pass through the filter. The concentrations of insulin-nanoparticle filtrate samples were then measured using BCA assay. Subtracting the concentration of filtrate samples from initial concentration of insulin at the start (0.2 mg), it was possible to quantify the concentration of insulin adsorbed on the surface of nanoparticles.

As shown in Figure 16, the amount of adsorbed insulin on the surface of amine-modified particles after 1 hour incubation at 65 °C is small whereas after 2 hours incubation, this amount had a considerable increase compared to one hour. The concentration of filtered insulin with no particles (negative control) after 1 or 2 hours of incubation was almost the same as the initial insulin concentration (0.2 mg/mL). Hence, it can be concluded that the reason that after 2 hours of incubation time the concentration of filtered insulin-particle was low is because most insulin proteins in the solution were adsorbed on the surface of particles.

Figure 16

Insulin adsorption on the surface of amine-modified polystyrene particles (200 nm). Incubation of insulin with concentration of 0.2 mg/mL at room temperature with the particles, at three different insulin to particle ratios (10000:1, 100:1, and 1:1), after 1 and 2 hours of incubation.

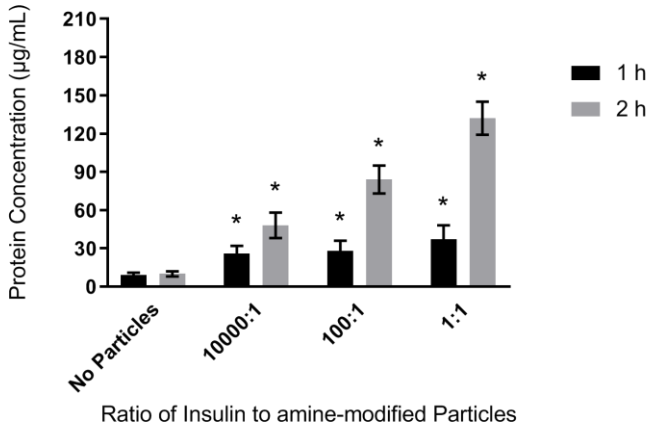

In case of insulin treated with sulfate-modified particle ratios of 1:1, 100:1 and 10000:1, after one hour of incubation time at 65 °C, relatively low protein adsorption on the surface of particles was recorded. Interestingly, protein adsorption on sulfate-modified nanoparticles with insulin ratio of 1:1 after two hours increased significantly (Figure 17). This indicates that almost all the insulin in the solution was adsorbed on particle surfaces.

Figure 17

Insulin adsorption on the surface of sub-micron sulfate-modified particles. Incubation of protein with concentration of 0.2 mg/mL at room temperature with sulfate-modified polystyrene (200 nm) particles at three different insulin-particle mass ratios (10000:1, 100:1, and 1:1) after 1 and 2 hours of protein incubation at 65 °C.

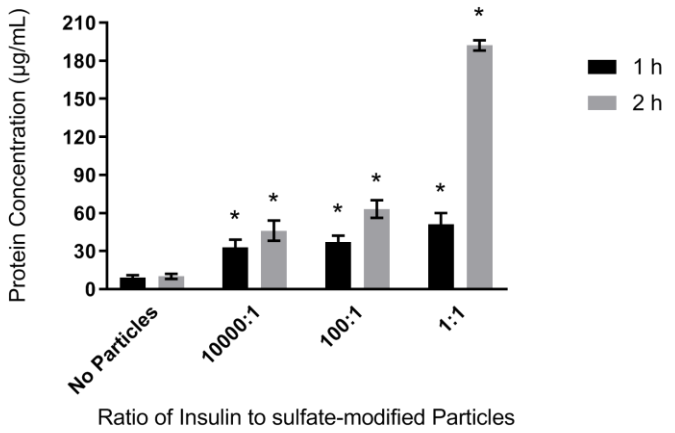

3.7 Circular Dichroism (CD) Spectrometry

CD spectrometry is an established method to estimate the secondary structure of proteins. This method is widely used to detect the presence of α helix and β sheet structures in proteins. CD spectra in the far-UV (below 260 nm) can also be used to predict the percentages of each secondary structure in a protein. CD spectra associated with some of the common protein secondary structures such as α-helix and β-sheet are shown in Figure 18.

Figure 18

Alpha-helix, β-sheet, and random coil structures each turn into a characteristic shape and magnitude of CD spectrum [72].

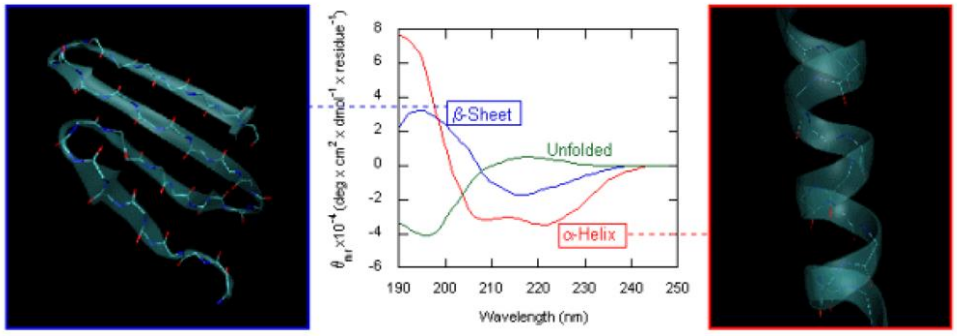

In order to study the mechanisms of fibril formation, changes in the secondary structure of insulin in the absence and the presence of nanoparticles (with an insulin-nanoparticle ratio of 1:1) were characterized. Studies have shown that misfolded proteins and aggregates are rich in the β-sheet structure [20],[11], [73]. Therefore, it was expected that more β-sheet structures would be detected as incubation at 65 ºC in acidic conditions proceeds. Mature fibrils formed after 4 hours were expected to show high extent of β-sheet formation. CD spectrum of pure human insulin shows negative peaks at 208 nm to 222 nm, indicating a mainly α-helical conformation [74] changes in the intensity of these bands or appearance of negative bands at 218 and 195 nm is a sign for the presence of β-sheet and disordered protein structure, respectively [74], [75].

Using CD, the spectra of diluted (0.1 mg/mL) insulin samples at different incubation time (t=1, 3, 4 hours) without nanoparticles, as control (Figure 19), and with amine and sulfate-modified nanoparticles with a protein: particle ratio of 1:1, wavelength between 190 and 260 nm, at room temperature was recorded (Figure 20 and 21). Insulin in the absence of particles after one hour of incubation at 65 ºC showed a negative band between 200 and 236 nm, confirming mainly α-helical structure. The same sample after 3- and 4-hours incubation time showed conformational changes indicating the formation of β-sheet structure. As shown in Figures 20 and 21, insulin samples containing amine and sulfate-modified particles also displayed conformational changes from α-helix (after 1 hour of incubation) to β-sheet (after 3 and 4 hours of incubation) confirming the existence of β-sheet structure. This finding was in agreement with literature reports that formation of fibrils is accompanied by the presence of β-sheet structures [10], [76], [77].

Figure 19

CD spectra of 0.1 mg/ml insulin in the absence of particles in HCl solution (pH 1.6) give temperature at time points of 1, 3, and 4 hours incubation time at 65 °C.

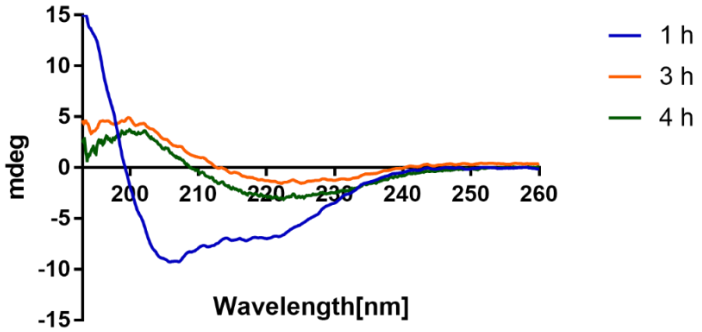

Figure 20

CD spectra of 0.1 mg/ml insulin fibrillation in HCl solution (pH 1.6) at time points of 1, 3, and 4 hours incubation time at 65 °C. Wavelength is between 190-260 nm. Graph represents CD spectra of insulin in presence of amine-modified polystyrene particles with ratios of 1:1 at various time points (1, 3, and 4 hours).

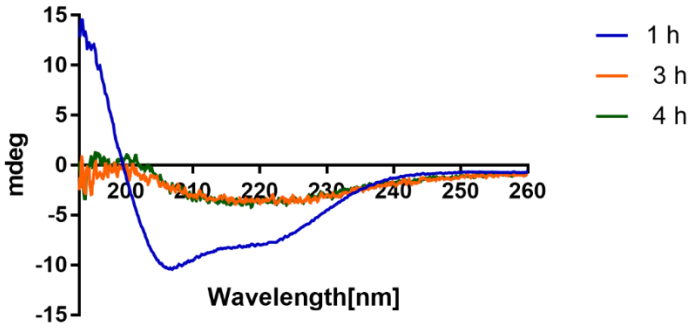

Figure 21

CD spectra of 0.1 mg/ml insulin fibrillation in HCl solution (pH 1.6) at time points of 1, 3, and 4 hours incubation time at 65 °C. Wavelength is between 190-260 nm. Graph represents CD spectra of insulin in presence of sulfate-modified polystyrene particles with ratios of 1:1 at various time points (1, 3, and 4 hours).

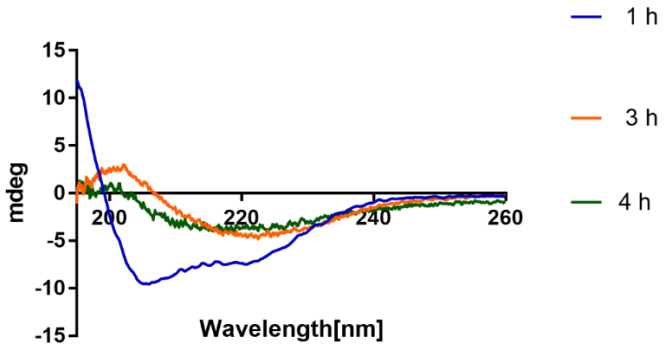

4. Discussion

4.1 Kinetics of Insulin Fibrillation

Insulin is a hexametric protein under physiological conditions, and it binds with two or four Zn^{+} ions [78]. In aqueous solutions at neutral pH, insulin is found to be in the hexamer form [79]. However *in vitro*, fibrillation of insulin from soluble proteins at neutral pH and at 37 ºC takes a few days to complete [5]. Some conditions including acidic environment, heat, and agitation, can disrupt the regular pattern of insulin assembly [80]–[82]. In acidic environment, molecules tend to undergo conformational changes, which creates a condition in which the attractive forces between the protein molecules is enhanced. As a result, the fibrillation rate of the protein is altered [80]. According to a study performed by Atta Ahmad et al, during the process of protein fibrillation, oligomers dissociate into monomers and monomers then undergo conformational changes and form partially folded intermediates. The aggregation of those partially-folded intermediates eventually leads to formation of insoluble amyloid fibrils [83]. Recent studies show that the occurrence of insulin amyloids in clinical situations is increasing [20], [18], [84]. Insulin amyloid-like fibrils can pose a variety of problems in biomedical and biotechnological applications, especially in insulin pumps being used for administration of insulin in the treatment of diabetes [20]. Insulin fibril deposition at the site of injection after repeated injection is also another problem occurring in patients with type II diabetes [20], [84]–[86].

Low pH (<2) which favors monomeric structures, along with temperatures >60 ºC induce the formation of fibrils over a period of a few hours [87]. In accordance, the majority of studies on insulin fibrillation have been performed under fibril inducing condition such as at a pH of 1.6 and at 65 ◦C [29], [34], [56] which are also the conditions used in the current study. Insulin fibrillation kinetics was examined using the ThT fluorescence assay [88]. ThT displays a shift in its excitation upon binding to protein structures with high β-sheet content [44]. Since protein aggressions are rich in β-sheet structures, this assay has been widely used to characterize protein aggregation [60], [89]. Fibrillation of insulin under these conditions demonstrated a well-known sigmoidal curve (Figure 10, orange line), which was in agreement with the literature [90], [91]. Three distinct phases, lag phase, elongation phase, and saturation phase could be clearly observed on this curve. During the lag phase, low fluorescence intensity values were recorded indicating the absence of mature fibrils and domination of insulin monomers and oligomers (consist of relatively few monomers). Due to a rapid increase in fluorescence intensity on the graph, a noticeable rise on graph was observed. This indicates the formation and growth of protofibrils, which corresponds to the elongation phase [92]. Following the elongation phase, the saturation phase is detected, during which fluorescence intensity reached a plateau as most oligomers and protofibrils have turned into mature fibrils.

Although insulin fibrillation rate was measured with the same protocol and under the same conditions for all the experiments, various lag times were observed. Three

different lag times were recorded including 1.5, 2, and 2.5 hours among which the 2-hour lag time was dominant. This could be because of the nature of insulin protein itself. Because of the inconsistency in the lag time, the lag times for sixteen experiment were measured and the average was calculated to be 2.19 ± 0.46 hours (n=16).

Considering this fact that ThT is able to bind to structures with high β-sheet content [44] and demonstrates enhanced fluorescence emission, formation of insulin fibrils was visualized by Fluorescence Microscopy (FM). As the amount of aggregations and fibrils increases in a solution, the fluorescent emitted by ThT enhances correspondingly. As Figure 8 displays the existence and the formation of fibrils at the beginning of nucleation/lag, elongation, and saturation phases, at t = 0 no aggregation or fibrillation exists. The aggregates started to form after 1.5 to 2.5 hours. By increasing the incubation time to 4 hours the aggregates were developed and became larger in size, which could be more visible by FM. In fact, by increasing the incubation time more aggregates were formed which subsequently developed into larger aggregations in form of fibrils. Therefore, the kinetics of the fibrillation process seems to be time dependent. Nielsen et al, explain the fibrillation behavior as a nucleation–elongation mechanism in which the lag time is the time needed for nuclei creation whereas fast fibrillation is as a result of monomer attachment to the ends of pre-existing fibrils [92]. The FM images of insulin samples at times 0, 2.5, and 4 hours were in agreement with the results recorded by the ThT assay and spectrofluorometer showing the kinetics of insulin fibrillation.

The effects of the presence of sub-micron particles on insulin fibrillation were investigated using sulfate- and amine-modified polystyrene beads (nominal diameter of 200 nm). The hydrodynamic size of sulfate- or amine-modified particles was 241 ± 12.2 and 223 ± 5.8 nm. While the particles had different surface-functional groups, they both showed a positive charge in the acidic medium (pH<2) used for insulin fibrillation. Sulfate and amine-modified particles, each one with three different protein-nanoparticle mass ratios of 10000:1, 100:1, and 1:1 was applied to study particle dose effects on the kinetics of insulin fibrillation. The results from fluorescence intensity of ThT represented no significant effect on insulin fibrillation in terms of the length of lag time and the rate of fibrillation once low protein-nanoparticle mass ratios of 10000:1, 100:1 was applied. On the other hand, by increasing the protein-particle weight ratio to 1:1 a significant effect on insulin fibrillation rate was observed. Both lag time and fibrillation rate were affected. Length of lag time was visibly shortened and an increased fluorescence intensity in the elongation and saturation phases was recorded. In summary, the presence of particles has altered insulin fibrillation kinetics. This effect was dose-dependent, but independent of particle surface properties. Low concentrations of amine-modified particles led to a slight, but statistically insignificant, increase in insulin fibrillation. However, at the highest particle to protein ratio of 1:1, the particles significantly increase the rate of fibrillation and resulted in increased fibril formation, as evidenced by increased fluorescence intensity at the end of fibrillation (Figure 11). Similar effects were observed with sulfate-modified particles at the highest concentration (Figure 10).

Importantly, the time required to complete the lag phase was significantly shortened in the presence of the particles at the highest concentration. The lag phase in the absence of particles was completed in 2.19 ± 0.46 hours. However, at the 1:1 protein to particle ratio, this time was significantly reduced to 1.16 ± 0.21 and 1.2 ± 0.27 hours for the sulfate- and amine-modified particles, respectively.

While nanoparticles were capable of altering insulin fibrillation behavior, this effect was highly dose-dependent and was only observed at a protein-particle weight ratio of 1:1. The accelerating effect of particles on the rate of insulin fibrillation was further confirmed by visually observing ThT-labeled fibrils using fluorescence microscopy (only the highest particle to protein ratio of 1:1 was used for these experiments, since particles had accelerated insulin fibrillation only at high concentration). In the presence of the particles, significantly faster fibrillation was observed, evidenced by the presence of fibrils after 1.5 hours of incubation with amine- or sulfate-modified particles (Figure 14) which visually confirmed the observations in Figure 10 and 11 representing insulin fibrillation in presence and absence of nanoparticles using ThT assay.

The fibrillation of insulin, and various other proteins, has been explained as a nucleation-elongation mechanism with the lag phase being the time required for the formation of stable nuclei [93]. It has been demonstrated that the presence of particles' surface enhances the rate of fibrillation likely due to the promotion of nucleation by the presence of the surface, which acts to increase the local concentration of proteins [94], [95]. In agreement, a number of studies have reported increased fibrillation of amyloid-

beta after exposure to nano-, or sub-micron particles in a dose-dependent manner, likely due to enhanced nucleation [54], [96], [97]. It should be noted that particle-induced inhibition of fibrillation has also been reported for both amyloid-beta [50], [98], [99] and insulin [34]. High concentration of particles provides a greater surface area for proteins to interact. Vicki et al. also explained the fibrillation induced by particles is due to large particle surface area as well as surface charge which promotes adsorption of the protein to the particle surface [39]. Other studies also described acceleration in fibril formation because of high local concentration of β2-microglobulin on copolymer particles, cerium oxide particles, quantum dots, and carbon nanotubes. The authors explain that fast fibrillation occurs because of "surface-assisted nucleation" by nanoparticles. They argue that formation of a nucleus is the most important rate-determining step in fibrillation. The adsorption of beta(2)-macroglobulin forms multiple layers on the particle surface creating an increased protein concentration which promotes nucleation and accelerates fibrillation [39], [66]. In the case of insulin, carbon dots were shown to have an inhibitory effect on fibrillation [34]. While the exact mechanism for the prevention of fibrillation was not determined, it was shown that particles inhibit fibrillation if added before a critical nucleus concentration, further suggesting that nucleation is a critical step in fibrillation.

Our results agree with the hypothesis that the presence of particles' surfaces facilitates fibrillation due to enhanced nucleation, evidenced by the shortened lag time of fibrillation once the particles are present (Figures 10, 11, and 14). However, while studies with ThT fluorescence suggest increased nucleation, these studies by themselves they do

not confirm the increased adsorption of proteins on particle surface, which is needed to promote nucleation. To further investigate whether faster fibrillation is caused by increased nucleation, the concentration of proteins on particle surfaces was examined.

4.2 Protein Adsorption on Particles' Surfaces

As discussed earlier, insulin fibrillation rate was accelerated as a result of insulin-nanoparticle interactions. Assuming that the adsorption of insulin on the surface of nanoparticles and formation of a nucleation site is the reason of fast fibrillation, BCA assay was applied to examine the amount of proteins on the surface of particles. Considering the fact that more adsorbed proteins on the surface of particles can create more chance of interaction between unfolded insulin monomers, which eventually develop into mature fibrils, if concentration of adsorbed proteins on the surface of particles is high, an increase in the fibrillation rate can be expected.

Amount of proteins adsorbed on particle surfaces was measured before the formation of fibrils (before lag time at t=0) and used as control when no aggregates were formed. To quantify the concentration of insulin on the surface of nanoparticles, a 10 mL insulin solution, with a concentration of 200 μg/mL (total protein content of 0.2 mg) was incubated with the particles (ratios of 1:1, 100:1, 10000:1) using the same conditions performed in the fibrillation experiments. Then, the protein-nanoparticle suspension was placed in an extruder and injected through 100 nm filters, resulting in the filtration of proteins that were not adsorbed on the surface of the particles. The amount of proteins on the surface of the particles, which were larger than the filter pore size and thus were not

filtered, was then estimated by measuring the total protein content using the BCA assay kit. By subtracting the concentration of filtrate samples from the initial concentration of insulin before incubation (0.2 mg); the concentration of insulin adsorbed on the surface of nanoparticles was quantified.

Protein adsorption on particle surfaces was both time- and dose-dependent. After one hour of incubation, as the ratio of protein to particles was increased from 10000:1 to 1:1, more protein was adsorbed on the surface of the particles as measured 33 ± 6, 51± 6 µg/mL, respectively. At two hours post-incubation, a more significant dose-dependent effect was observed. For example, concentration of adsorbed insulin proteins after two hours at a protein to particle ratio of 10000:1 was measured to be 46 ± 8 and 48 ± 10 µg/mL on the surface of sulfate- and amine-modified particles, respectively. However, at a particle to protein ratio of 1:1 the amount of adsorbed protein was increased to 132 ± 13 µg/mL and 192 ± 4 µg/mL for the amine- and sulfate-modified particles, respectively (Figures 16 and 17). Protein adsorption on particle surfaces was strongly time-dependent with a significant increase in the amount of adsorbed proteins observed at two hours, compared to one-hour, post-incubation. For example, in case of protein to particle ratio of 1:1, insulin protein concentration on the surface of sulfate-modified particles after one hour and two hours incubation time has been increased from 51 ± 6 to 192 ± 4 µg/mL. The concentration of adsorbed insulin on the surface of amine-modified particles after 1-hour incubation at 65 °C is small whereas after 2 hours incubation, this increases remarkably compared to one hour. As a negative control, the concentration of filtered

insulin with no particles was also measured after one or two hours of incubation. As those concentrations (0.194 ± 0.3 and 0.192 ± 0.3 mg/mL) were almost the same as the initial insulin concentration (0.2 mg/mL), it can be concluded that the low concentration of filtered insulin-particle ratio of 1:1 after 2 hours is because of high protein adsorption on the surface of particles. Once insulin was treated with sulfate-modified particles ratios of 1:1, 100:1 and 10000:1, after 1-hour incubation time at 65 °C, relatively low protein adsorption on the surface of particles was recorded. Interestingly, protein adsorption on sulfate-modified nanoparticles with insulin ratio of 1:1 after 2 hours increased significantly. The concentration of adsorbed protein on surface of nanoparticles in the case of insulin-particle with weight ratio of 1:1 after two hours of incubation is very close to the initial concentration of insulin which indicates that almost all insulin proteins in the solution have been adsorbed. It is worth mentioning that at two hours post-incubation, sulfate-modified particles adsorbed more proteins compared to amine-modified nanoparticles. The zeta potential of insulin (before fibrillation at t=0), amine-modified, and sulfate-modified at pH 1.6 were measured as 17.4 ± 2.4, 21.7 ± 1.3, and 3.5 ± 0.4 mV, respectively. Therefore, more adsorbed protein on sulfate-modified particles could be due to less repulsive forces or more affinity between insulin proteins and sulfate-modified particles, compared to amine-modified and insulin over the two-hour post-incubation time at pH 1.6. This strongly supports the idea that high local concentration of proteins can act as a potential nucleation site for insulin proteins which subsequently increases interaction and boosts fibrillation rate [8], [13]. Overall, the results from the

protein adsorption studies strongly suggest that particles increase the local concentration of proteins and thus serve as a potential nucleation site for insulin as has been previously suggested for other proteins [7], [13], [14].

4.3 Protein Secondary Structure after Exposure to Particles

Particle-induced alterations in protein fibrillation behavior are associated with changes in the protein secondary structure [10], [101]–[103]. Formation of protein fibrils involves a change in the protein secondary structure to β-sheets. Consequently, particles that induce fibrillation result in an increase in the β-sheet structure, while particles that inhibit fibrillation favor alpha-helix structure [99]. There is a direct relationship between β-sheet formation and fibrillation and particles that inhibit the fibrillation lag time of insulin have been shown to do so by inhibiting the change in the secondary structure from alpha-helix to β-sheet [34]. To investigate how particles, affect protein secondary structure, far UV-CD was employed. For these studies, protein secondary structure was investigated after 1, 3, or 4 hours of incubation at 65℃ at pH of 1.6 with and without particles. Only the highest particle concentration (1:1) was chosen for this experiment as only in this case fast fibrillation was recorded.

Insulin showed primarily α-helical structure after one hour of incubation in fibril-inducing conditions without particles. This was evidenced by the presence of negative bands at 208 nm and 222 nm, which are hallmarks of α-helical structure and have been used to confirm insulin α-helices [5 and 38]. In the presence of amine-modified particles, no significant changes in insulin secondary structure were observed at one-hour post-

incubation. At three- or four-hours post-incubation, insulin showed a β-sheet structure with or without the particles evidenced by the presence of a broad minimum at ~220 nm. Overall, the CD experiments suggest that while β-sheet formation was observed after protein fibrillation with or without particles. The presence of particles might have led to an earlier onset of β-sheet formation which is in agreement with the observations in the fibrillation kinetics studies. After 4 hours incubation time with particles there was no considerable change in the secondary structure.

5. Conclusion

Due to their large surface-to-volume ratio, nanoparticles show significant adsorptive behavior and are suitable for binding with drugs, probes, chemical compounds, and proteins. Recent studies show increasing interest in using engineered nanoparticles to detect and prevent diseases caused by misfolded proteins [51], [56], [91], [104], [105]. Various researches have investigated the effects of nanoparticles on protein fibrillation *in vitro*, showing the ability of engineered nanoparticles to alter protein fibrillation behavior [29], [30], [32], with an emphasis on amyloid beta, the misfolded protein associated with Alzheimer's disease [32], [33], [106], [107].

The current research aimed to study on the effect of nanoparticles on insulin fibril formation process. Insulin fibrillation has been reported to be mainly due to altering the nucleation phase of fibrillation, thus particles may enhance or retard fibrillation process [7]. Factors such as changes in pH, ionic strength, anions, and stabilizers can impact the lag time and fibril growth formation, which indicates the significance of hydrophobic and electrostatic interactions in the nucleation phase [32]. These information gives an insight that nanoparticles with various surface chemistries may be able to interfere with the nucleation phase and subsequently affect the fibrillation process.

In this study, first, insulin fibrillation was studied and then the effects of polystyrene sub-micron particles with different surface functionalities on the fibrillation behavior of human insulin were investigated using ThT assay. The amount of the fluorescent emitted by ThT corresponds to the amount of fibrils formed in a solution.

This tendency of ThT to bind to fibrils was used to visually examine fibril formation over time. Using the ThT assay, three stages were observed in insulin fibrillation profile: a lag phase, an elongation phase, and a saturation phase. Although all the experiments were performed under the same conditions and with the same protocol, variable lag times, between 1.5 to 2.5 hours were recorded while the fibrillation profile was the same. Changes in lag time were likely due to slight changes in pH, as has been previously reported in the literature [46], [47]. Fluorescence microscopy was used to monitor and visualize the formation of aggregates and fibrils during fibrillation. Microscopy images of samples at time 0, 2.5, and 4 hours were in agreement with the results recorded by ThT assay and spectrofluorometer. AFM and confocal microscopy were also used to visualize the morphology of mature fibrils. The AFM image showed that, long insulin fibrils were appeared in samples after 4 h incubation at 65 ^{o}C. Fibrils were long, straight and unbranched, in agreement with literature data.

To study the effect of nanoparticles on insulin fibrillation, polystyrene particles with a nominal diameter of 200 nm and with two different surface chemistries, amine- and sulfate-modified, were applied, at three particle to protein mass ratios of 1:1, 100:1, and 10000:1. Our results demonstrate that regardless of the functional group, nanoparticles with the lowest concentration did not substantially affect insulin fibrillation in terms of the length of lag time and the amount of fibrils. Increasing the concentration of sulfate-modified particles to protein-particle weight ratio of 100:1 still showed no considerable effect on insulin fibrillation rate. However, at a higher protein-particle

weight ratio of 1:1, the lag time was visibly shortened, and more fluorescence intensity recorded at each point of time, suggesting an increase in the amount of fibrils. The presence of sulfate-particles led to faster fibrillation than amine-modified particles. In general, both amine- and sulfate-modified particles promoted insulin fibrillation in a dose-dependent manner, with significant increase in the rate of fibrillation observed only when the proteins and particles are present at the same mass ratio (1:1). These effects were confirmed with fluorescence microscopy and support our hypothesis that the surface of the particles encourage the nucleation process and facilitates fibrillation as evidenced by the shortened lag time.

To further investigate the adsorption of proteins on particle surface and also estimate the concentration of proteins on the surface of particles, BCA assay was employed. Concentration of adsorbed proteins on the surface of amine- and sulfate-modified particles (ratios of 1:1, 100:1 and 10000:1) was measured after one and two hours incubation at 65 °C. Based on the results, the amount of insulin adsorbed on the surface of amine-modified particles after 1 hour of incubation at 65 °C was small whereas after two hours incubation, this amount showed a considerable increase. In case of insulin treated with sulfate-modified particles with ratios of 1:1, almost all of insulin in the solution was adsorbed on the surface of nanoparticles after two hours, further suggesting that nanoparticles can act as a nucleation site for proteins to form fibrils. Results from CD spectra also indicated that insulin samples containing amine and sulfate-modified particles (ratio of 1:1) undergo a conformational changes from α-helix (after one hour of

incubation) to β-sheet (after three and four hours of incubation) confirming the existence of β-sheet structure. As fibrils are rich in β-sheet structure, existence of insulin fibrils is concluded. These findings are important in understanding the role of sub-micron particles in controlling insulin fibrillogenesis either during production or transfer of the protein or due to unwanted exposure.

6. Future Work

As mentioned earlier, insulin is composed of two polypeptide chains (A and B), and these two chains are linked by three disulfate bonds. In the current study, the secondary structure of insulin amyloid fibrils was investigated by Circular Dichroism, but there is still room for studying the status of these disulfate bonds during the fibrillation process. The partial reduction is a widely accepted method for the determination of disulfate bonds. In this approach, insulin fibrils can be further analyzed by Mass Spectrometry (MS) and/or tandem MS. Knowing the status of disulfide bonds can give more information and a better insight into the structure of insulin amyloid fibrils during fibrillation process.

The morphology of mature insulin fibrils in the absence of nanoparticles were characterized in this study by AFM. However, more information is needed regarding the morphology of insulin fibrils in the presence of amine and sulfate-modified particles particularly with protein-particle mass ratio of 1:1. Since amine and sulfate-modified particles (ratio of 1:1) substantially increased the fluorescence intensity at the saturation phase, it needs to be elucidated if this high intensity is because of larger aggregations, smaller but more frequent aggregates, or both. AFM images from samples of insulin treated with particles after four hours of incubation could answer this question and provide valuable information about the structure of the fibrils in presence of particles.

In this study, the effect of amine- and sulfate-modified polystyrene particles on insulin fibrillation was investigated. However, the effect of these particles can be studied on fibrillation of another known protein such as amyloid beta as well. These nanoparticles can act differently with other kinds of proteins and have a distinct effect on the fibrillation rate. Unlike insulin, amyloid-beta consists of only one polypeptide chain with 36–43 amino acids. Due to the difference in the structure of a protein and the sequence of amino acids particles can interact differently and produce a distinct result. The same weight ratios of amyloid beta-particles 1:1, 100:1, and 10000:1 can be applied, and then the fibrillation profile and rate can be monitored.

Another avenue worth pursuing is investigation into the effect of biocompatible particles on insulin fibrillation. Therefore, the same weight ratios of protein-particles (1:1, 100:1, and 10000:1) can be applied to study insulin fibrillation behavior. We can also try and switch between different particle to find one being able to inhibit fibrillation. Being biocompatible and having an inhibitory effect on fibrillation, those particles could be considered as a potential option for dealing with insulin fibrillation *in vivo*. Poly(lactic-co-glycolic acid) (PLGA) is one of the well-known biodegradable and biocompatible polymeric particles, approved by the US Food and Drug Administration (FDA) for medical applications [109] could be a great candidate for such a study.

References

[1] Z. Khosravi, S. Sharma, and A. M. Farnoud, "Submicron polymeric particles accelerate insulin fibrillation by surface adsorption," *Biointerphases*, vol. 14, no. 2, p. 021001, Mar. 2019, doi: 10.1116/1.5083821.

[2] P. Cuatrecasas, S. Jacobs, and J. Avruch, *Insulin*. Berlin; New York: Springer-Verlag, 1990.

[3] G. Wilcox, "Insulin and Insulin Resistance," *Clin. Biochem. Rev.*, vol. 26, no. 2, pp. 19–39, May 2005.

[4] M. J. Adams *et al.*, "Structure of Rhombohedral 2 Zinc Insulin Crystals," *Nature*, vol. 224, no. 5218, Art. no. 5218, Nov. 1969, doi: 10.1038/224491a0.

[5] C. Iannuzzi, M. Borriello, M. Portaccio, G. Irace, and I. Sirangelo, "Insights into Insulin Fibril Assembly at Physiological and Acidic pH, and Related Amyloid Intrinsic Fluorescence," *Int. J. Mol. Sci.*, vol. 18, no. 12, Nov. 2017, doi: 10.3390/ijms18122551.

[6] "Protein structure: Primary, secondary, tertiary and quaternary (article)," *Khan Academy*. https://www.khanacademy.org/science/biology/macromolecules/proteins-and-amino-acids/a/orders-of-protein-structure (accessed Jul. 16, 2020).

[7] B. Alberts, A. Johnson, J. Lewis, M. Raff, K. Roberts, and P. Walter, "The Shape and Structure of Proteins," *Mol. Biol. Cell 4th Ed.*, 2002, Accessed: Jul. 15, 2020. [Online]. Available: https://www.ncbi.nlm.nih.gov/books/NBK26830/.

[8] C. M. Dobson, "Protein folding and misfolding," *Nature*, vol. 426, no. 6968, pp. 884–890, Dec. 2003, doi: 10.1038/nature02261.

[9] C. M. Dobson, "Protein-misfolding diseases: Getting out of shape," *Nature*, vol. 418, no. 6899, pp. 729–730, Aug. 2002, doi: 10.1038/418729a.

[10] R. N. Rambaran and L. C. Serpell, "Amyloid fibrils," *Prion*, vol. 2, no. 3, pp. 112–117, 2008.

[11] E. I. Agorogiannis, G. I. Agorogiannis, A. Papadimitriou, and G. M. Hadjigeorgiou, "Protein misfolding in neurodegenerative diseases," *Neuropathol. Appl. Neurobiol.*, vol. 30, no. 3, pp. 215–224, Jun. 2004, doi: 10.1111/j.1365-2990.2004.00558.x.

[12] G. B. Irvine, O. M. El-Agnaf, G. M. Shankar, and D. M. Walsh, "Protein Aggregation in the Brain: The Molecular Basis for Alzheimer's and Parkinson's Diseases," *Mol. Med.*, vol. 14, no. 7–8, pp. 451–464, 2008, doi: 10.2119/2007-00100.Irvine.

[13] C. A. Ross and M. A. Poirier, "Protein aggregation and neurodegenerative disease," *Nat. Med.*, vol. 10 Suppl, pp. S10-17, Jul. 2004, doi: 10.1038/nm1066.

[14] P. Westermark *et al.*, “Amyloid in polypeptide hormone-producing tumors,” *Lab. Investig. J. Tech. Methods Pathol.*, vol. 37, no. 2, pp. 212–215, Aug. 1977.

[15] P. Westermark, C. Wernstedt, E. Wilander, D. W. Hayden, T. D. O’Brien, and K. H. Johnson, “Amyloid fibrils in human insulinoma and islets of Langerhans of the diabetic cat are derived from a neuropeptide-like protein also present in normal islet cells,” *Proc. Natl. Acad. Sci. U. S. A.*, vol. 84, no. 11, pp. 3881–3885, Jun. 1987.

[16] “Protein aggregation: Pathways, induction factors and analysis - Mahler - 2009 - Journal of Pharmaceutical Sciences - Wiley Online Library.” https://onlinelibrary.wiley.com/doi/10.1002/jps.21566 (accessed Jul. 15, 2020).

[17] M. Muzaffar and A. Ahmad, “The Mechanism of Enhanced Insulin Amyloid Fibril Formation by NaCl Is Better Explained by a Conformational Change Model,” *PLoS ONE*, vol. 6, no. 11, Nov. 2011, doi: 10.1371/journal.pone.0027906.

[18] S. Yumlu, R. Barany, M. Eriksson, and C. Röcken, “Localized insulin-derived amyloidosis in patients with diabetes mellitus: a case report,” *Hum. Pathol.*, vol. 40, no. 11, pp. 1655–1660, Nov. 2009, doi: 10.1016/j.humpath.2009.02.019.

[19] S. Okamura, Y. Hayashino, S. Kore-Eda, and S. Tsujii, “Localized Amyloidosis at the Site of Repeated Insulin Injection in a Patient With Type 2 Diabetes,” *Diabetes Care*, vol. 36, no. 12, pp. e200–e200, Dec. 2013, doi: 10.2337/dc13-1651.

[20] F. E. Dische *et al.*, “Insulin as an amyloid-fibril protein at sites of repeated insulin injections in a diabetic patient,” *Diabetologia*, vol. 31, no. 3, pp. 158–161, Mar. 1988, doi: 10.1007/BF00276849.

[21] A. Serrano-Pozo, M. P. Frosch, E. Masliah, and B. T. Hyman, “Neuropathological Alterations in Alzheimer Disease,” *Cold Spring Harb. Perspect. Med.*, vol. 1, no. 1, Sep. 2011, doi: 10.1101/cshperspect.a006189.

[22] P. Barranco Morales, “Kinetics of human and bovine insulin amyloid fibril formation in the presence of solid/liquid interfaces,” *Masters Theses*, Jan. 2013, [Online]. Available: https://scholarsmine.mst.edu/masters_theses/7193.

[23] R. Khurana *et al.*, “A General Model for Amyloid Fibril Assembly Based on Morphological Studies Using Atomic Force Microscopy,” *Biophys. J.*, vol. 85, no. 2, pp. 1135–1144, Aug. 2003.

[24] J. L. Jiménez, E. J. Nettleton, M. Bouchard, C. V. Robinson, C. M. Dobson, and H. R. Saibil, “The protofilament structure of insulin amyloid fibrils,” *Proc. Natl. Acad. Sci. U. S. A.*, vol. 99, no. 14, pp. 9196–9201, Jul. 2002, doi: 10.1073/pnas.142459399.

[25] J. Juárez, P. Taboada, and V. Mosquera, “Existence of Different Structural Intermediates on the Fibrillation Pathway of Human Serum Albumin,” *Biophys. J.*, vol. 96, no. 6, pp. 2353–2370, Mar. 2009, doi: 10.1016/j.bpj.2008.12.3901.

[26] L. Breydo and V. N. Uversky, “Chapter 1 - Molecular Mechanisms of Protein Misfolding,” in *Bio-nanoimaging*, V. N. Uversky and Y. L. Lyubchenko, Eds. Boston: Academic Press, 2014, pp. 1–14.

[27] “Chapter 3_Modeling Amyloid Fibrillation.pdf.” Accessed: Jul. 15, 2020. [Online]. Available: http://web.mit.edu/mcraegroup/wwwfiles/ChuangChuang/thesis_files/Chapter%203_Modeling%20Amyloid%20Fibrillation.pdf.

[28] P. C. Ke *et al.*, “Implications of peptide assemblies in amyloid diseases,” *Chem. Soc. Rev.*, vol. 46, no. 21, pp. 6492–6531, Oct. 2017, doi: 10.1039/C7CS00372B.

[29] E. Kachooei, A. A. Moosavi-Movahedi, F. Khodagholi, H. Ramshini, F. Shaerzadeh, and N. Sheibani, “Oligomeric forms of insulin amyloid aggregation disrupt outgrowth and complexity of neuron-like PC12 cells,” *PloS One*, vol. 7, no. 7, p. e41344, 2012, doi: 10.1371/journal.pone.0041344.

[30] “Nucleation-dependent fibril formation process.,” *ResearchGate*. https://www.researchgate.net/figure/Nucleation-dependent-fibril-formation-process_fig2_248384536 (accessed Jul. 15, 2020).

[31] T. Tomiyama *et al.*, “Inhibition of Amyloid Protein Aggregation and Neurotoxicity by Rifampicin ITS POSSIBLE FUNCTION AS A HYDROXYL RADICAL SCAVENGER,” *J. Biol. Chem.*, vol. 271, no. 12, pp. 6839–6844, Mar. 1996, doi: 10.1074/jbc.271.12.6839.

[32] S. I. Yoo *et al.*, “Inhibition of amyloid peptide fibrillation by inorganic nanoparticles: functional similarities with proteins,” *Angew. Chem. Int. Ed Engl.*, vol. 50, no. 22, pp. 5110–5115, May 2011, doi: 10.1002/anie.201007824.

[33] L. Xiao, D. Zhao, W.-H. Chan, M. M. F. Choi, and H.-W. Li, “Inhibition of beta 1-40 amyloid fibrillation with N-acetyl-L-cysteine capped quantum dots,” *Biomaterials*, vol. 31, no. 1, pp. 91–98, Jan. 2010, doi: 10.1016/j.biomaterials.2009.09.014.

[34] S. Li *et al.*, “Nontoxic Carbon Dots Potently Inhibit Human Insulin Fibrillation,” *Chem. Mater.*, vol. 27, no. 5, pp. 1764–1771, Mar. 2015, doi: 10.1021/cm504572b.

[35] T. Wang, X. Ma, Y. Lei, and Y. Luo, “Solid lipid nanoparticles coated with cross-linked polymeric double layer for oral delivery of curcumin,” *Colloids Surf. B Biointerfaces*, vol. 148, pp. 1–11, Dec. 2016, doi: 10.1016/j.colsurfb.2016.08.047.

[36] I. Lynch, T. Cedervall, M. Lundqvist, C. Cabaleiro-Lago, S. Linse, and K. A. Dawson, “The nanoparticle-protein complex as a biological entity; a complex fluids and surface science challenge for the 21st century,” *Adv. Colloid Interface Sci.*, vol. 134–135, pp. 167–174, Oct. 2007, doi: 10.1016/j.cis.2007.04.021.

[37] W. Ma *et al.*, “Modular assembly of proteins on nanoparticles,” *Nat. Commun.*, vol. 9, no. 1, Art. no. 1, Apr. 2018, doi: 10.1038/s41467-018-03931-4.

[38] C. Cabaleiro-Lago *et al.*, “Inhibition of amyloid beta protein fibrillation by polymeric nanoparticles,” *J. Am. Chem. Soc.*, vol. 130, no. 46, pp. 15437–15443, Nov. 2008, doi: 10.1021/ja8041806.

[39] C. Vl and K. Km, “Nanoparticles as catalysts for protein fibrillation.,” *Proc. Natl. Acad. Sci. U. S. A.*, vol. 104, no. 21, pp. 8679–8680, May 2007, doi: 10.1073/pnas.0703194104.

[40] S. Linse *et al.*, “Nucleation of protein fibrillation by nanoparticles,” *Proc. Natl. Acad. Sci. U. S. A.*, vol. 104, no. 21, pp. 8691–8696, May 2007, doi: 10.1073/pnas.0701250104.

[41] M. Zaman, E. Ahmad, A. Qadeer, G. Rabbani, and R. H. Khan, “Nanoparticles in relation to peptide and protein aggregation,” *Int. J. Nanomedicine*, vol. 9, pp. 899–912, Feb. 2014, doi: 10.2147/IJN.S54171.

[42] “Protein–nanoparticle interactions: main factors that can affect...,” *ResearchGate*. https://www.researchgate.net/figure/Protein-nanoparticle-interactions-main-factors-that-can-affect-proteins-resulting-in_fig3_41453783 (accessed Jul. 15, 2020).

[43] P. S. Vassar and C. F. Culling, “Fluorescent stains, with special reference to amyloid and connective tissues,” *Arch. Pathol.*, vol. 68, pp. 487–498, Nov. 1959.

[44] M. Biancalana and S. Koide, “Molecular Mechanism of Thioflavin-T Binding to Amyloid Fibrils,” *Biochim. Biophys. Acta*, vol. 1804, no. 7, pp. 1405–1412, Jul. 2010, doi: 10.1016/j.bbapap.2010.04.001.

[45] M. H. Shin and H.-S. Lim, “Screening methods for identifying pharmacological chaperones,” *Mol. Biosyst.*, vol. 13, no. 4, pp. 638–647, Mar. 2017, doi: 10.1039/C6MB00866F.

[46] I. W. Hamley, “The amyloid beta peptide: a chemist’s perspective. Role in Alzheimer’s and fibrillization,” *Chem. Rev.*, vol. 112, no. 10, pp. 5147–5192, Oct. 2012, doi: 10.1021/cr3000994.

[47] W.-H. Wu *et al.*, “TiO2 nanoparticles promote beta-amyloid fibrillation in vitro,” *Biochem. Biophys. Res. Commun.*, vol. 373, no. 2, pp. 315–318, Aug. 2008, doi: 10.1016/j.bbrc.2008.06.035.

[48] G. Thakur *et al.*, “Conjugated Quantum Dots Inhibit the Amyloid β (1–42) Fibrillation Process,” *Int. J. Alzheimers Dis.*, vol. 2011, Mar. 2011, doi: 10.4061/2011/502386.

[49] C. E. Giacomelli and W. Norde, “Influence of hydrophobic Teflon particles on the structure of amyloid beta-peptide,” *Biomacromolecules*, vol. 4, no. 6, pp. 1719–1726, Dec. 2003, doi: 10.1021/bm034151g.

[50] K. A. Moore *et al.*, “Influence of gold nanoparticle surface chemistry and diameter upon Alzheimer’s disease amyloid-β protein aggregation.,” *J. Biol. Eng.*, vol. 11, pp. 5–5, 2017, doi: 10.1186/s13036-017-0047-6.

[51] E. A. Elbassal *et al.*, “Gold Nanoparticles as a Probe for Amyloid-β Oligomer and Amyloid Formation,” *J. Phys. Chem. C Nanomater. Interfaces*, vol. 121, no. 36, pp. 20007–20015, Sep. 2017, doi: 10.1021/acs.jpcc.7b05169.

[52] H. Skaat, R. Chen, I. Grinberg, and S. Margel, “Engineered polymer nanoparticles containing hydrophobic dipeptide for inhibition of amyloid-β fibrillation,” *Biomacromolecules*, vol. 13, no. 9, pp. 2662–2670, Sep. 2012, doi: 10.1021/bm3011177.

[53] M. Mahmoudi *et al.*, “Influence of the Physiochemical Properties of Superparamagnetic Iron Oxide Nanoparticles on Amyloid β Protein Fibrillation in Solution,” *ACS Chem. Neurosci.*, vol. 4, no. 3, pp. 475–485, Mar. 2013, doi: 10.1021/cn300196n.

[54] C. Cabaleiro-Lago, F. Quinlan-Pluck, I. Lynch, K. A. Dawson, and S. Linse, “Dual effect of amino modified polystyrene nanoparticles on amyloid β protein fibrillation,” *ACS Chem. Neurosci.*, vol. 1, no. 4, pp. 279–287, Apr. 2010, doi: 10.1021/cn900027u.

[55] Y. Sun and D. Hu, “The link between diabetes and atrial fibrillation: cause or correlation?,” *J. Cardiovasc. Dis. Res.*, vol. 1, no. 1, pp. 10–11, 2010, doi: 10.4103/0975-3583.59978.

[56] H. Skaat, M. Sorci, G. Belfort, and S. Margel, “Effect of maghemite nanoparticles on insulin amyloid fibril formation: selective labeling, kinetics, and fibril removal by a magnetic field,” *J. Biomed. Mater. Res. A*, vol. 91, no. 2, pp. 342–351, Nov. 2009, doi: 10.1002/jbm.a.32232.

[57] A. Sukhanova, S. Poly, A. Shemetov, and I. Nabiev, “Quantum dots induce charge-specific amyloid-like fibrillation of insulin at physiological conditions,” *Prog. Biomed. Opt. Imaging - Proc. SPIE*, vol. 8548, Oct. 2012, doi: 10.1117/12.946606.

[58] H. G, M. A, S. Aa, and M.-M. Aa, “Unfolding of insulin at the surface of ZnO quantum dots.,” *Int. J. Biol. Macromol.*, vol. 86, pp. 169–176, Jan. 2016, doi: 10.1016/j.ijbiomac.2016.01.075.

[59] R. Yousefi, S. Jalili, P. Alavi, and A.-A. Moosavi-Movahedi, “The enhancing effect of homocysteine thiolactone on insulin fibrillation and cytotoxicity of insulin fibril,” *Int. J. Biol. Macromol.*, vol. 51, no. 3, pp. 291–298, Oct. 2012, doi: 10.1016/j.ijbiomac.2012.05.021.

[60] L. Nh *et al.*, “Examining the effects of dextran-based polymer-coated nanoparticles on amyloid fibrillogenesis of human insulin.,” *Colloids Surf. B Biointerfaces*, vol. 172, pp. 674–683, Sep. 2018, doi: 10.1016/j.colsurfb.2018.09.029.

[61] A. Zhou, J. Xie, H. Han, Y. Chen, C. Zhao, and J. Li, “Supramolecular Nanoparticles of Insulin and Pentapeptide for Inhibition of Fibrillation, and Controlled Release,” *J. Biomed. Nanotechnol.*, vol. 14, no. 5, pp. 959–967, May 2018, doi: 10.1166/jbn.2018.2550.

[62] “3159-zetasizer-nano-user-manual-englishpdf.pdf.” Accessed: Jun. 30, 2020. [Online]. Available: https://www.ursinus.edu/live/files/3159-zetasizer-nano-user-manual-englishpdf.

[63] P. K. Smith *et al.*, “Measurement of protein using bicinchoninic acid,” *Anal. Biochem.*, vol. 150, no. 1, pp. 76–85, Oct. 1985, doi: 10.1016/0003-2697(85)90442-7.

[64] A. K. Attri, C. Fernández, and A. P. Minton, “pH-dependent self-association of zinc-free Insulin characterized by concentration-gradient static light scattering,” *Biophys. Chem.*, vol. 148, no. 1–3, pp. 28–33, May 2010, doi: 10.1016/j.bpc.2010.02.002.

[65] M. F. Dunn, “Zinc-ligand interactions modulate assembly and stability of the insulin hexamer -- a review,” *Biometals Int. J. Role Met. Ions Biol. Biochem. Med.*, vol. 18, no. 4, pp. 295–303, Aug. 2005, doi: 10.1007/s10534-005-3685-y.

[66] E. J. Nettleton, P. Tito, M. Sunde, M. Bouchard, C. M. Dobson, and C. V. Robinson, “Characterization of the Oligomeric States of Insulin in Self-Assembly and Amyloid Fibril Formation by Mass Spectrometry,” *Biophys. J.*, vol. 79, no. 2, pp. 1053–1065, Aug. 2000, doi: 10.1016/S0006-3495(00)76359-4.

[67] F. Chiti and C. M. Dobson, “Protein misfolding, functional amyloid, and human disease,” *Annu. Rev. Biochem.*, vol. 75, pp. 333–366, 2006, doi: 10.1146/annurev.biochem.75.101304.123901.

[68] Y. Xu, Y. Yan, D. Seeman, L. Sun, and P. L. Dubin, “Multimerization and aggregation of native-state insulin: effect of zinc,” *Langmuir ACS J. Surf. Colloids*, vol. 28, no. 1, pp. 579–586, Jan. 2012, doi: 10.1021/la202902a.

[69] C. Cabaleiro-Lago, O. Szczepankiewicz, and S. Linse, “The Effect of Nanoparticles on Amyloid Aggregation Depends on the Protein Stability and Intrinsic Aggregation Rate,” *Langmuir*, vol. 28, no. 3, pp. 1852–1857, Jan. 2012, doi: 10.1021/la203078w.

[70] E. Kachooei, A. A. Moosavi-Movahedi, F. Khodagholi, H. Ramshini, F. Shaerzadeh, and N. Sheibani, “Oligomeric Forms of Insulin Amyloid Aggregation Disrupt Outgrowth and Complexity of Neuron-Like PC12 Cells,” *PLOS ONE*, vol. 7, no. 7, p. e41344, Jul. 2012, doi: 10.1371/journal.pone.0041344.

[71] “Chemistry of Protein Assays - US.” //www.thermofisher.com/us/en/home/life-science/protein-biology/protein-biology-learning-center/protein-biology-resource-library/pierce-protein-methods/chemistry-protein-assays.html (accessed Jul. 16, 2020).

[72] “cd.pdf.” Accessed: Jun. 23, 2020. [Online]. Available: http://www.sbs.ntu.edu.sg/interactions/Documents/cd.pdf.

[73] S. Gregoire, J. Irwin, and I. Kwon, “Techniques for Monitoring Protein Misfolding and Aggregation in Vitro and in Living Cells,” *Korean J. Chem. Eng.*, vol. 29, no. 6, pp. 693–702, Jun. 2012, doi: 10.1007/s11814-012-0060-x.

[74] N. J. Greenfield, “Using circular dichroism spectra to estimate protein secondary structure,” *Nat. Protoc.*, vol. 1, no. 6, pp. 2876–2890, 2006, doi: 10.1038/nprot.2006.202.

[75] “Circular Dichroism Techniques: Biomolecular and Nanostructural Analyses- A Review - Ranjbar - 2009 - Chemical Biology and amp; Drug Design - Wiley Online Library.” https://onlinelibrary.wiley.com/doi/full/10.1111/j.1747-0285.2009.00847.x (accessed Jul. 16, 2020).

[76] V. N. Uversky and Y. Lyubchenko, *Bio-nanoimaging: Protein Misfolding and Aggregation*. Academic Press, 2013.

[77] C. Sachse, M. Fändrich, and N. Grigorieff, “Paired β-sheet structure of an Aβ(1-40) amyloid fibril revealed by electron microscopy,” *Proc. Natl. Acad. Sci. U. S. A.*, vol. 105, no. 21, pp. 7462–7466, May 2008, doi: 10.1073/pnas.0712290105.

[78] J. A. G. Pertusa *et al.*, “Zn2+ chelation by serum albumin improves hexameric Zn2+-insulin dissociation into monomers after exocytosis,” *PLoS ONE*, vol. 12, no. 11, Nov. 2017, doi: 10.1371/journal.pone.0187547.

[79] X. Chang, A. M. Jorgensen, P. Bardrum, and J. J. Led, “Solution structures of the R6 human insulin hexamer,” *Biochemistry*, vol. 36, no. 31, pp. 9409–9422, Aug. 1997, doi: 10.1021/bi9631069.

[80] J. L. Whittingham *et al.*, “Insulin at pH 2: structural analysis of the conditions promoting insulin fibre formation,” *J. Mol. Biol.*, vol. 318, no. 2, pp. 479–490, Apr. 2002, doi: 10.1016/S0022-2836(02)00021-9.

[81] M. T. Mawhinney, T. L. Williams, J. L. Hart, M. L. Taheri, and B. Urbanc, “Elucidation of insulin assembly at acidic and neutral pH: Characterization of low

molecular weight oligomers," *Proteins*, vol. 85, no. 11, pp. 2096–2110, Nov. 2017, doi: 10.1002/prot.25365.

[82] Q. Zheng and N. D. Lazo, "Mechanistic Studies of the Inhibition of Insulin Fibril Formation by Rosmarinic Acid," *J. Phys. Chem. B*, vol. 122, no. 8, pp. 2323–2331, Mar. 2018, doi: 10.1021/acs.jpcb.8b00689.

[83] A. Ahmad, I. S. Millett, S. Doniach, V. N. Uversky, and A. L. Fink, "Partially Folded Intermediates in Insulin Fibrillation," *Biochemistry*, vol. 42, no. 39, pp. 11404–11416, Oct. 2003, doi: 10.1021/bi034868o.

[84] S. Okamura, Y. Hayashino, S. Kore-Eda, and S. Tsujii, "Localized Amyloidosis at the Site of Repeated Insulin Injection in a Patient With Type 2 Diabetes," *Diabetes Care*, vol. 36, no. 12, p. e200, Dec. 2013, doi: 10.2337/dc13-1651.

[85] Y. Shikama *et al.*, "Localized amyloidosis at the site of repeated insulin injection in a diabetic patient," *Intern. Med. Tokyo Jpn.*, vol. 49, no. 5, pp. 397–401, 2010.

[86] S. Yumlu, R. Barany, M. Eriksson, and C. Röcken, "Localized insulin-derived amyloidosis in patients with diabetes mellitus: a case report," *Hum. Pathol.*, vol. 40, no. 11, pp. 1655–1660, Nov. 2009, doi: 10.1016/j.humpath.2009.02.019.

[87] J. Brange, L. Andersen, E. D. Laursen, G. Meyn, and E. Rasmussen, "Toward understanding insulin fibrillation," *J. Pharm. Sci.*, vol. 86, no. 5, pp. 517–525, May 1997, doi: 10.1021/js960297s.

[88] M. M. Wördehoff and W. Hoyer, "α-Synuclein Aggregation Monitored by Thioflavin T Fluorescence Assay," *Bio-Protoc.*, vol. 8, no. 14, Jul. 2018, doi: 10.21769/BioProtoc.2941.

[89] A.-W. Lee, C.-C. Hsu, Y.-Z. Liu, P.-L. Wei, and J.-K. Chen, "Supermolecules of poly(N-isopropylacrylamide) complexating Herring sperm DNA with bio-multiple hydrogen bonding," *Colloids Surf. B Biointerfaces*, vol. 148, pp. 422–430, Dec. 2016, doi: 10.1016/j.colsurfb.2016.09.015.

[90] S. Li *et al.*, "Nontoxic Carbon Dots Potently Inhibit Human Insulin Fibrillation," *Chem. Mater.*, vol. 27, no. 5, pp. 1764–1771, Mar. 2015, doi: 10.1021/cm504572b.

[91] Q. Q. Yang *et al.*, "Active site-targeted carbon dots for the inhibition of human insulin fibrillation," *J. Mater. Chem. B*, vol. 5, no. 10, pp. 2010–2018, Mar. 2017, doi: 10.1039/C6TB02823C.

[92] C.-C. Lee, A. Nayak, A. Sethuraman, G. Belfort, and G. J. McRae, "A Three-Stage Kinetic Model of Amyloid Fibrillation," *Biophys. J.*, vol. 92, no. 10, pp. 3448–3458, May 2007, doi: 10.1529/biophysj.106.098608.

[93] L. Nielsen *et al.*, “Effect of environmental factors on the kinetics of insulin fibril formation: elucidation of the molecular mechanism,” *Biochemistry*, vol. 40, no. 20, pp. 6036–6046, May 2001.

[94] A. N. Nayak, A. Dutta, and G. Belfort, “Surface-enhanced nucleation of insulin amyloid fibrillation,” *Biochem. Biophys. Res. Commun.*, vol. 369, pp. 303–7, Jun. 2008, doi: 10.1016/j.bbrc.2008.01.159.

[95] F. Librizzi and C. Rischel, “The kinetic behavior of insulin fibrillation is determined by heterogeneous nucleation pathways,” *Protein Sci. Publ. Protein Soc.*, vol. 14, no. 12, pp. 3129–3134, Dec. 2005, doi: 10.1110/ps.051692305.

[96] S. Linse *et al.*, “Nucleation of protein fibrillation by nanoparticles,” *Proc. Natl. Acad. Sci. U. S. A.*, vol. 104, no. 21, pp. 8691–8696, May 2007, doi: 10.1073/pnas.0701250104.

[97] W. H. Wu *et al.*, “TiO2 nanoparticles promote beta-amyloid fibrillation in vitro.,” *Biochem. Biophys. Res. Commun.*, vol. 373, no. 2, pp. 315–318, Aug. 2008, doi: 10.1016/j.bbrc.2008.06.035.

[98] L. Xiao, D. Zhao, W. H. Chan, M. M. Choi, and H. W. Li, “Inhibition of beta 1-40 amyloid fibrillation with N-acetyl-L-cysteine capped quantum dots.,” *Biomaterials*, vol. 31, no. 1, pp. 91–98, Jan. 2010, doi: 10.1016/j.biomaterials.2009.09.014.

[99] S. Rocha, A. F. Thünemann, M. do C. Pereira, M. Coelho, H. Möhwald, and G. Brezesinski, “Influence of fluorinated and hydrogenated nanoparticles on the structure and fibrillogenesis of amyloid beta-peptide,” *Biophys. Chem.*, vol. 137, no. 1, pp. 35–42, Sep. 2008, doi: 10.1016/j.bpc.2008.06.010.

[100] S. Linse *et al.*, “Nucleation of protein fibrillation by nanoparticles,” *Proc. Natl. Acad. Sci. U. S. A.*, vol. 104, no. 21, pp. 8691–8696, May 2007, doi: 10.1073/pnas.0701250104.

[101] J. Greenwald and R. Riek, “Biology of Amyloid: Structure, Function, and Regulation,” *Structure*, vol. 18, no. 10, pp. 1244–1260, Oct. 2010, doi: 10.1016/j.str.2010.08.009.

[102] C. G. Glabe, “Common mechanisms of amyloid oligomer pathogenesis in degenerative disease,” *Neurobiol. Aging*, vol. 27, no. 4, pp. 570–575, Apr. 2006, doi: 10.1016/j.neurobiolaging.2005.04.017.

[103] C. Iannuzzi, R. Maritato, G. Irace, and I. Sirangelo, “Misfolding and Amyloid Aggregation of Apomyoglobin,” *Int. J. Mol. Sci.*, vol. 14, no. 7, pp. 14287–14300, Jul. 2013, doi: 10.3390/ijms140714287.

[104] H. Skaat, G. Shafir, and S. Margel, “Acceleration and inhibition of amyloid-β fibril formation by peptide-conjugated fluorescent-maghemite nanoparticles,” *J.*

Nanoparticle Res., vol. 13, no. 8, pp. 3521–3534, Aug. 2011, doi: 10.1007/s11051-011-0276-4.

[105] D. Sun *et al.*, "Design of PLGA-functionalized quercetin nanoparticles for potential use in Alzheimer's disease," *Colloids Surf. B Biointerfaces*, vol. 148, pp. 116–129, Dec. 2016, doi: 10.1016/j.colsurfb.2016.08.052.

[106] "Effect of maghemite nanoparticles on insulin amyloid fibril formation: Selective labeling, kinetics, and fibril removal by a magnetic field - Skaat - 2009 - Journal of Biomedical Materials Research Part A - Wiley Online Library." https://onlinelibrary.wiley.com/doi/full/10.1002/jbm.a.32232 (accessed Oct. 16, 2018).

[107] N.-H. Lu *et al.*, "Examining the effects of dextran-based polymer-coated nanoparticles on amyloid fibrillogenesis of human insulin," *Colloids Surf. B Biointerfaces*, vol. 172, pp. 674–683, Sep. 2018, doi: 10.1016/j.colsurfb.2018.09.029.

[108] Y. Xu, Y. Yan, D. Seeman, L. Sun, and P. L. Dubin, "Multimerization and aggregation of native-state insulin: effect of zinc," *Langmuir ACS J. Surf. Colloids*, vol. 28, no. 1, pp. 579–586, Jan. 2012, doi: 10.1021/la202902a.

[109] A. Pandey, "Poly Lactic-Co-Glycolic Acid (PLGA) Copolymer and Its Pharmaceutical Application," 2015, pp. 151–172.

Thesis and Dissertation Services